

# Study of high-spin states by using stable and unstable nuclear beams

Eiji Ideguchi  
CNS, the University of Tokyo

# Contents

---

- Introduction of high-spin studies
- Stable nuclear beam experiments
  - Study of superdeformation and beyond
    - = Limit of high-spin, deformation
  - Gamma-ray spectroscopy near  $^{100}\text{Sn}$ 
    - = Limit of proton-rich study
- Unstable nuclear beam experiments
  - In-beam gamma-ray spectroscopy
- Future prospects

# Introduction

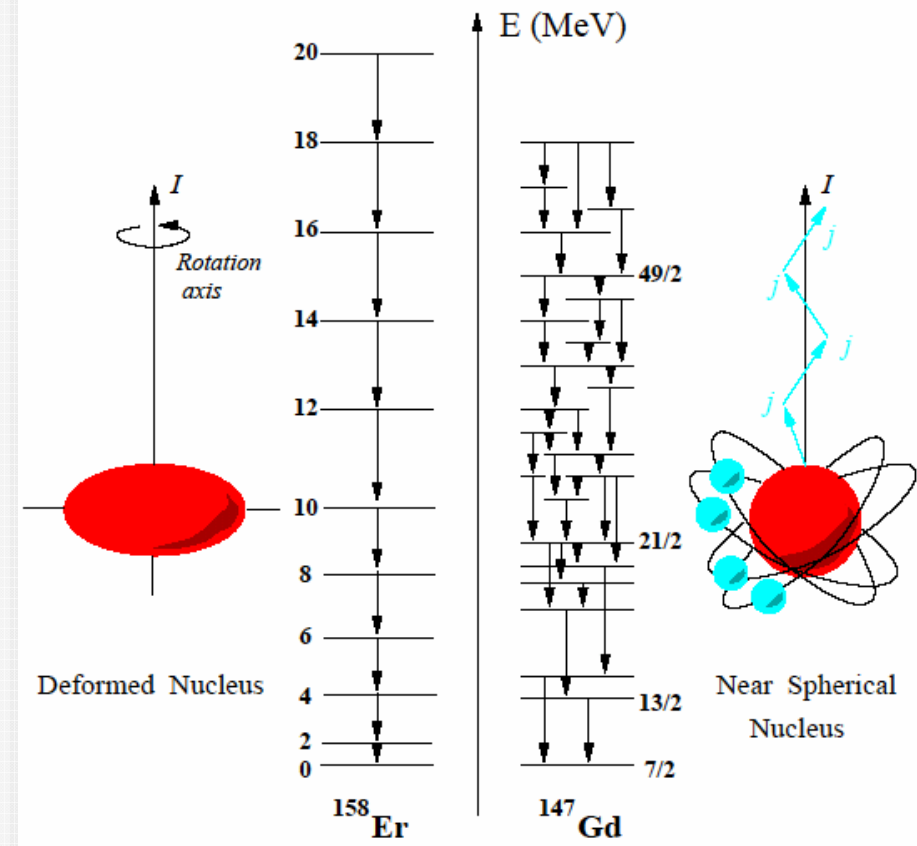
Change of nuclear structure  
in the excited state

as a function  $\downarrow$  of angular  
momentum  $\downarrow$

High-spin states

$\downarrow$   
Two basic aspects of  
nuclear motion

1. Single-particle motion  
 $\rightarrow$  Shell model
2. Collective motion  
 $\rightarrow$  Liquid drop model



# Nuclei at the limits

---

- Limit of angular momentum

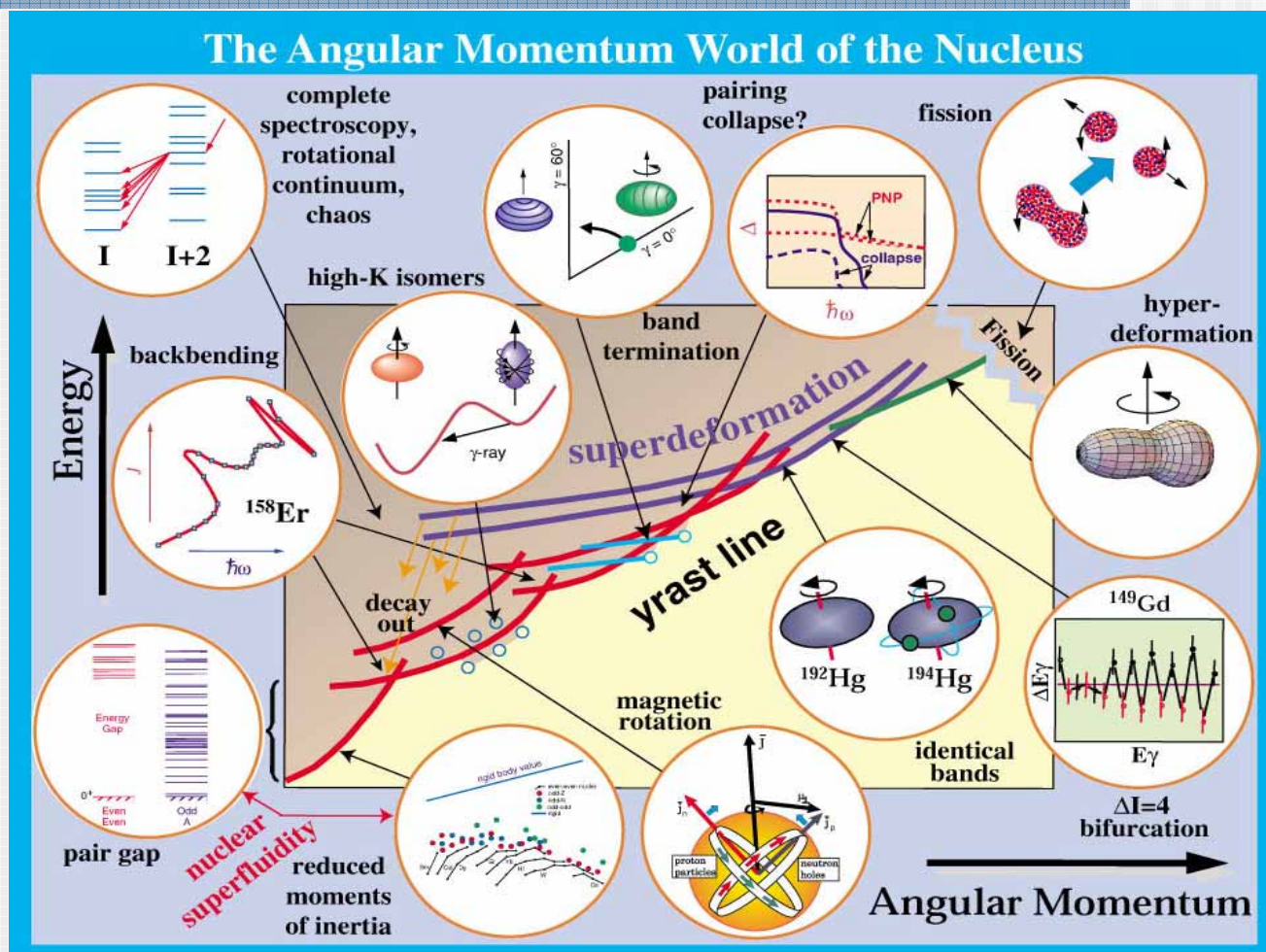
The question of the maximal angular momentum that a nucleus is able to sustain against rotation is an old and still unsolved problem

- Limit of deformation

superdeformation, hyperdeformation

- Limit of isospin (proton-rich)

# Behavior of nucleus at high-spin



# Limits of angular momentum and band termination

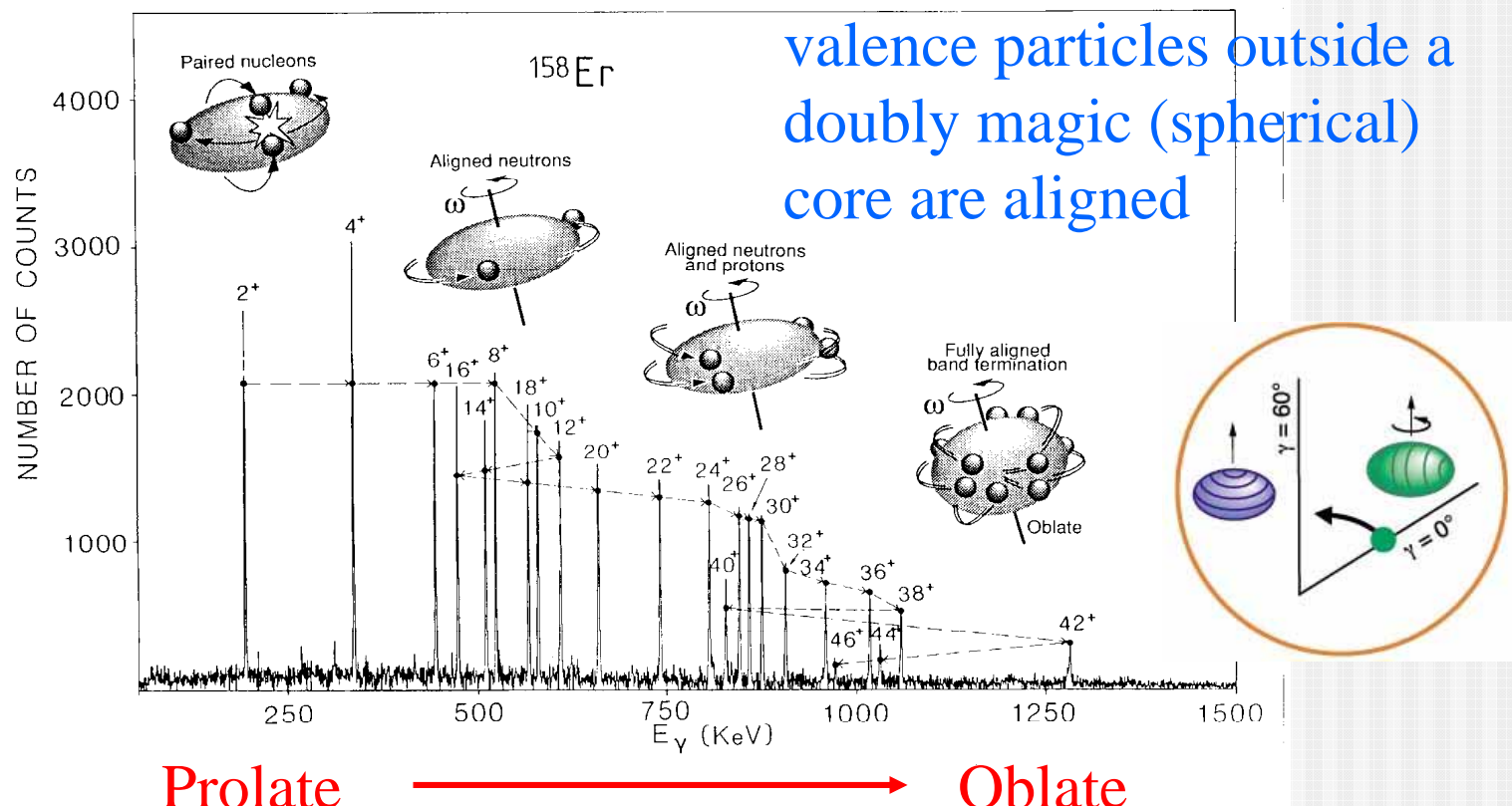
---

- Nuclear angular momentum is generated by the finite number of constituent nucleons
- Maximum number of angular momentum for a given nucleus with specific configuration
- This is seen as **termination of a rotational band** in nuclei when the nuclear angular momentum is generated entirely from constituent of nucleons rather than collective excitation

# Yrast band of $^{158}\text{Er}$

## High-spin of deformed nucleus

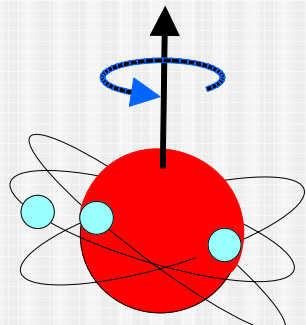
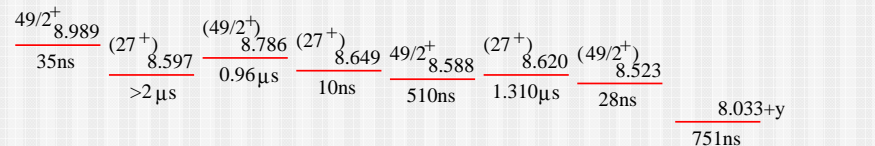
Simpson et al., Phys. Rev. Lett. 53(1984)648



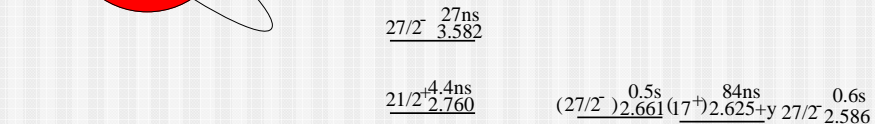
Yrast: lowest energy at given angular momentum

# High-spin isomer (oblate shape)

Oblate:  $\beta \sim -0.19$

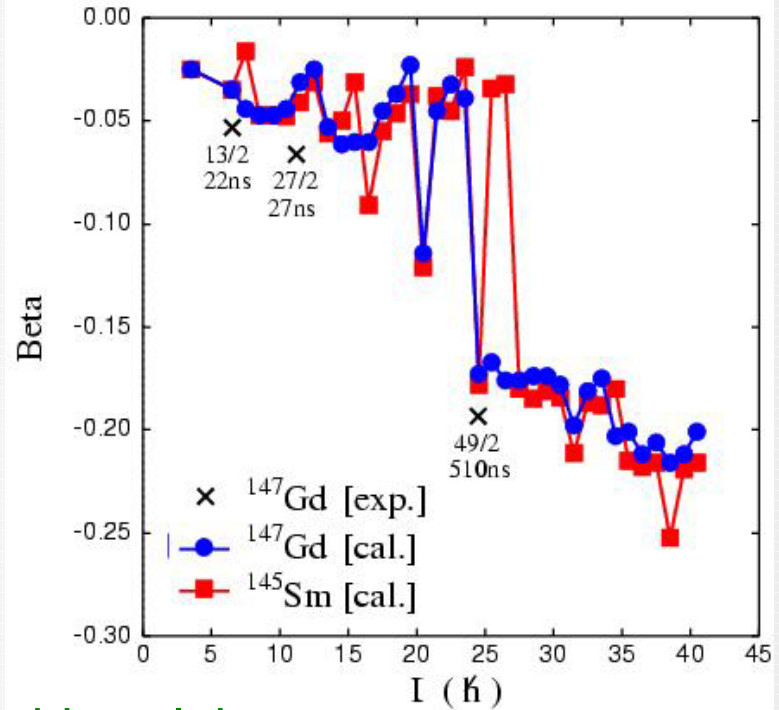


$N=83$  isotone



$5.750\text{ns}$	$11^-$	$\beta = 1.769$ , $\tau = 4.5\text{ns}$
$5.750\text{ns}$	$11^-$	$\beta = 1.769$ , $\tau = 4.5\text{ns}$
$1.228$	$13/2^-$	$\beta = 1.105$ , $\tau = 0.71\mu\text{s}$
$9^+$	$9^+$	$\beta = 0.841$ , $\tau = 0.71\mu\text{s}$
$9^+$	$9^+$	$\beta = 0.841$ , $\tau = 0.71\mu\text{s}$
stable	$5^-$	$\beta = 0.841$ , $\tau = 0.71\mu\text{s}$
$143_{60}\text{Nd}$	$144_{61}\text{Pm}$	$145_{62}\text{Sm}$
$146_{63}\text{Eu}$	$147_{64}\text{Gd}$	$148_{65}\text{Tb}$
$149_{66}\text{Dy}$	$150_{67}\text{Ho}$	$151_{68}\text{Er}$

High-spin states of spherical nucleus



odd nuclei

$$[\nu (f_{7/2} h_{9/2} i_{13/2}) \pi h_{11/2}^2]_{49/2}^+$$

odd-odd nuclei

$$[\nu (f_{7/2} h_{9/2} i_{13/2}) \pi (h_{11/2}^2 d_{5/2})]_{27}^+$$

# How to study high-spin states

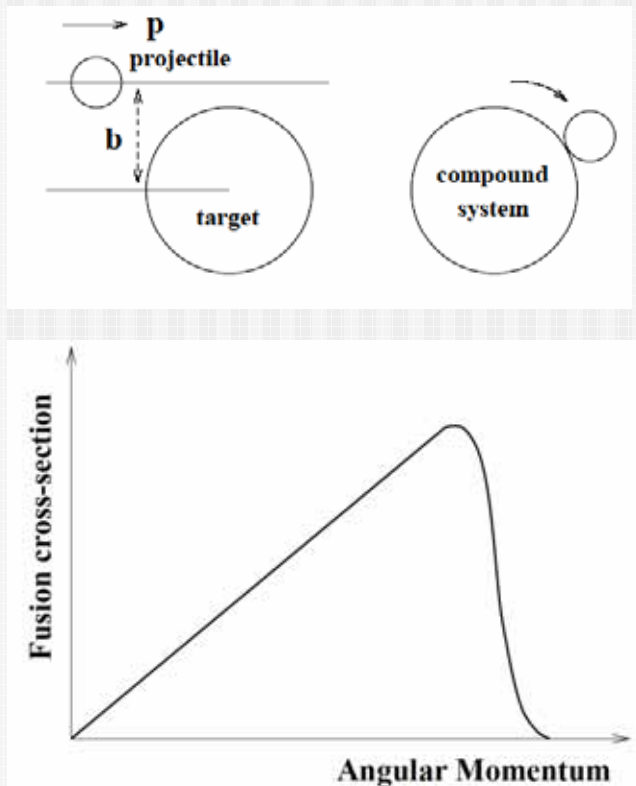
- Fusion-evaporation reaction
- Coulomb excitation
- Transfer reaction ( $^{18}\text{O}$ ,  $^{16}\text{O}$ )
- Fragmentation
- Fission

Spontaneous:  $^{238}\text{U}$ ,  $^{244,246,248}\text{Cm}$ ,  
 $^{250,252}\text{Cf}$ ,  $^{253}\text{Es}$ ,  $^{254,256}\text{Fm}$

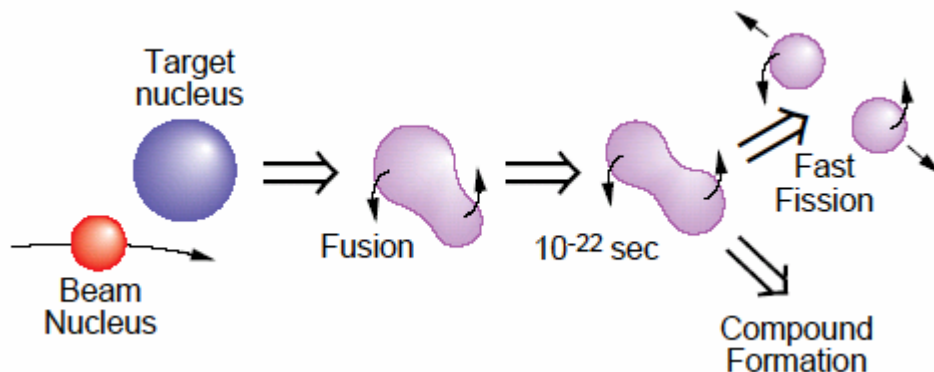
n-induced:  $^{235}\text{U}(n,f)$

- $\beta$  decay

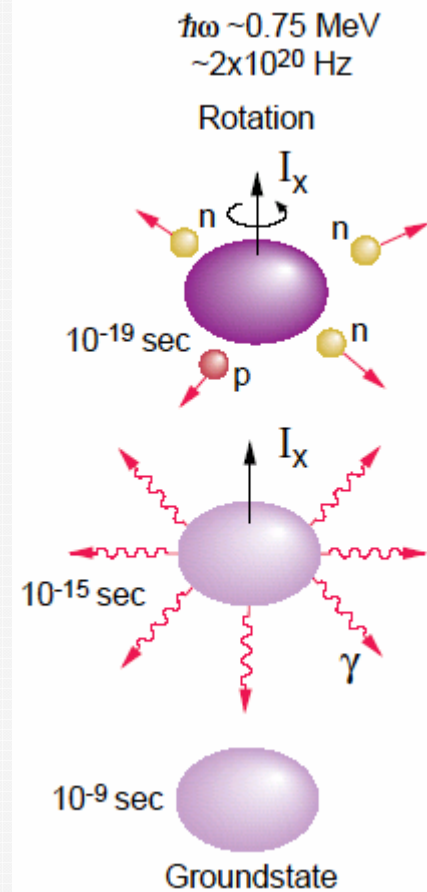
$$\ell = \mathbf{b} \times \mathbf{p}$$
$$d\sigma_{\text{fus}}(\ell) \propto \ell$$



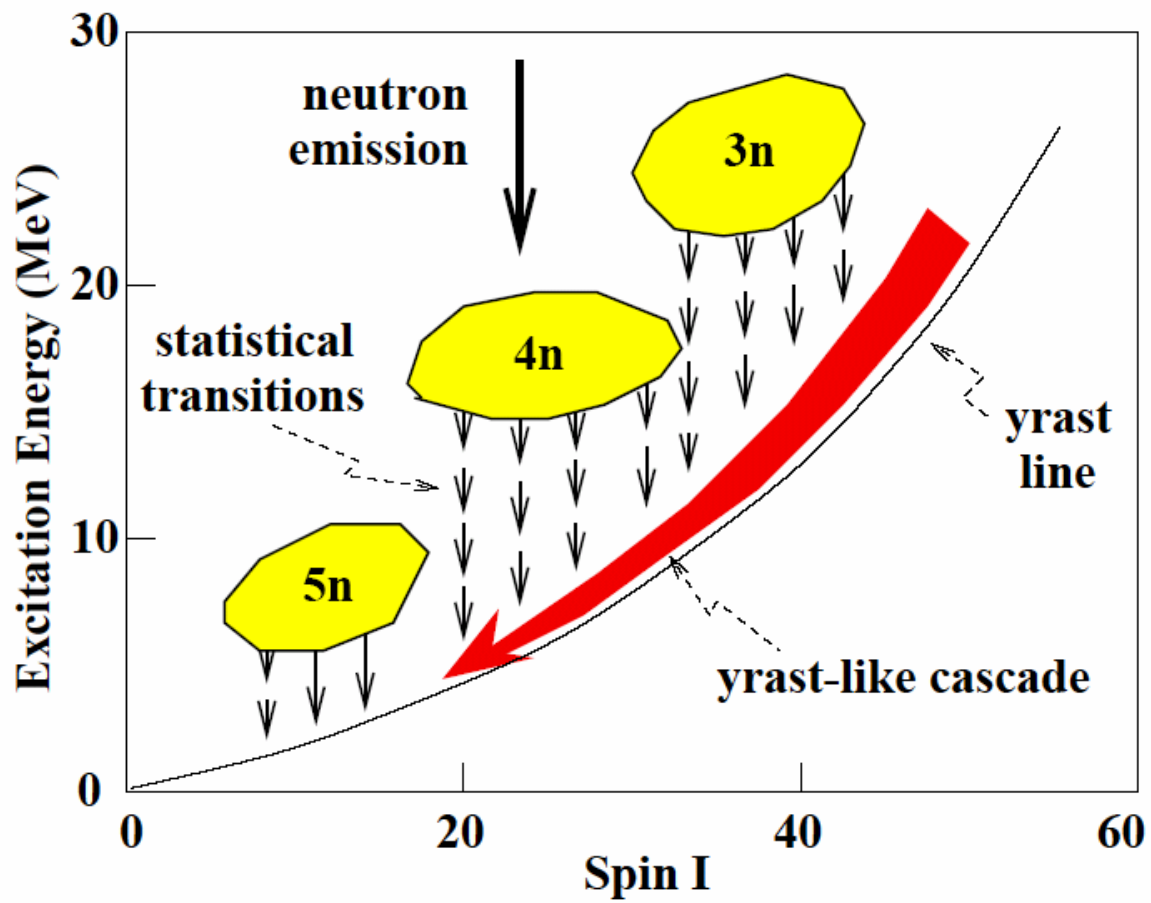
# Fusion-evaporation reaction



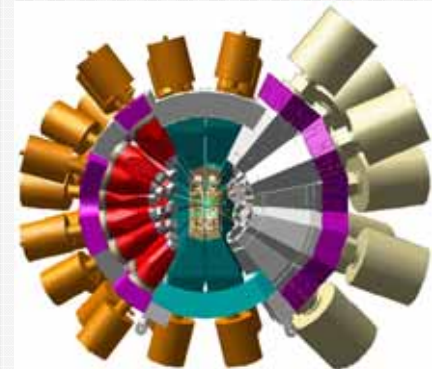
3-6 MeV/A



# Fusion evaporation and gamma decay



Measure  
Gamma decay  
To investigate  
High-spin excited  
states



Euroball

# High-spin limit

---

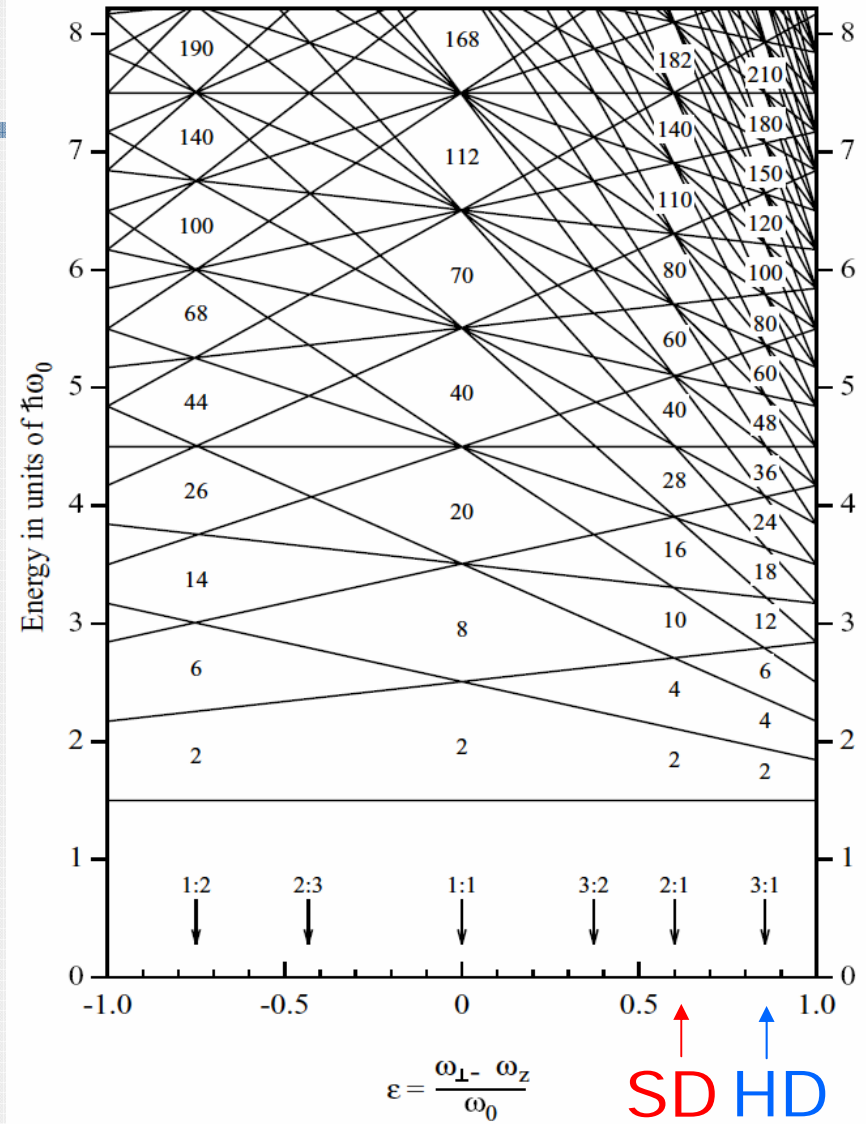
- For small deformed nucleus, configurations will terminate into a non-collective oblate state where the spin is given by the sum of angular momenta of single particle configuration:  $I_{\max}$
- For large deformation (superdeformation), spin above  $I_{\max}$  can be generated
- With increasing angular momentum, large deformed states (superdeformation, hyperdeformation) become yrast, and finally will decay by fission

# Superdeformed shell gaps

H.O.    Realistic  
            Potential

- $140 \Leftrightarrow \sim 146$  fission isomer
- $110 \Leftrightarrow 112 \quad A=190 (N)$
- $80 \Leftrightarrow 80 \sim 82 \quad A=190 (Z)$
- $60 \Leftrightarrow \sim 64 \quad A=150 (Z)$
- $40 \Leftrightarrow 42 \quad A=80$
- $28 \Leftrightarrow 30 \quad A=60$
- $16 \Leftrightarrow 16 \quad S$

K.Matsuyanagi,  
RIKEN winter  
school 2002



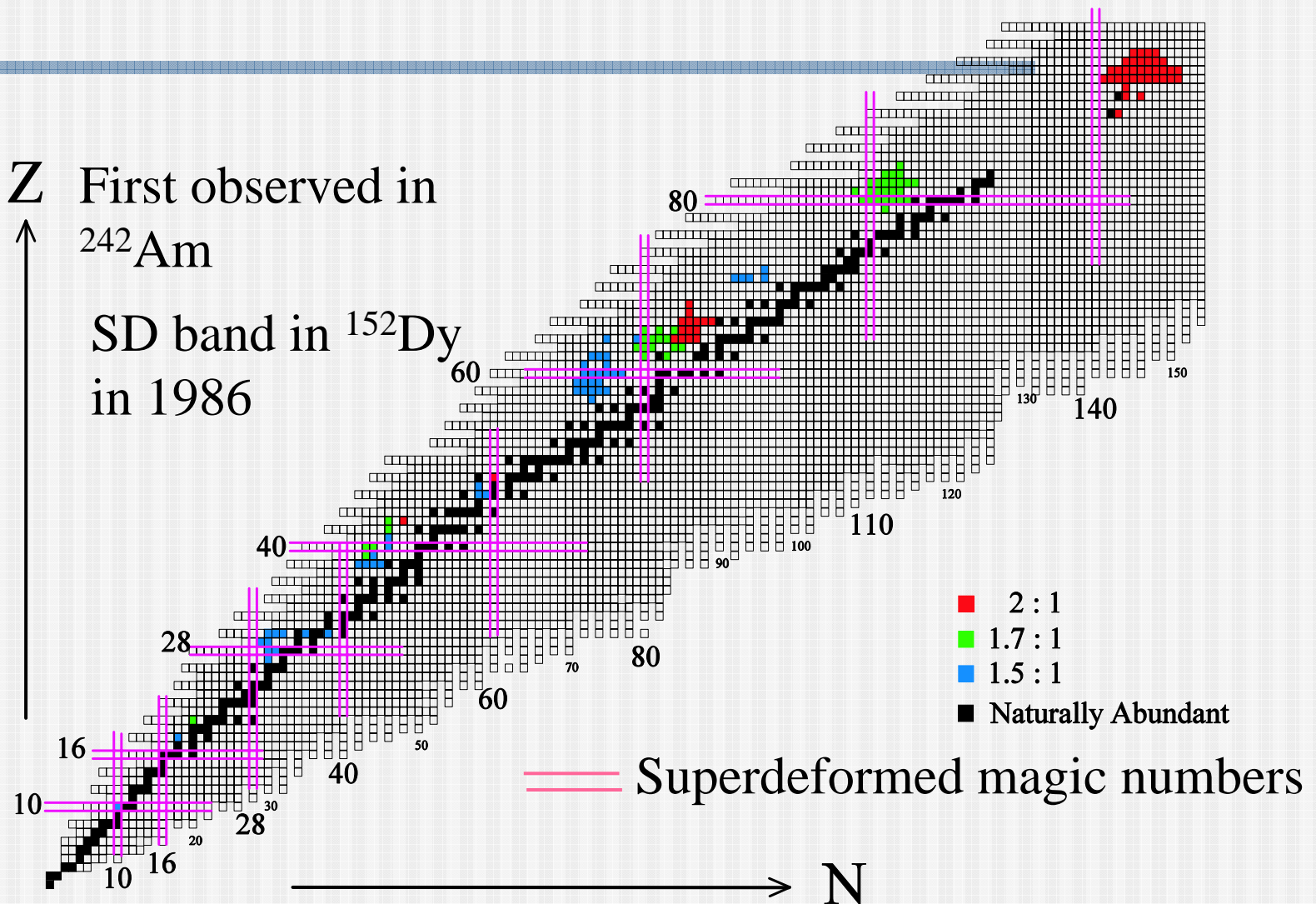
# Superdeformation

2:1

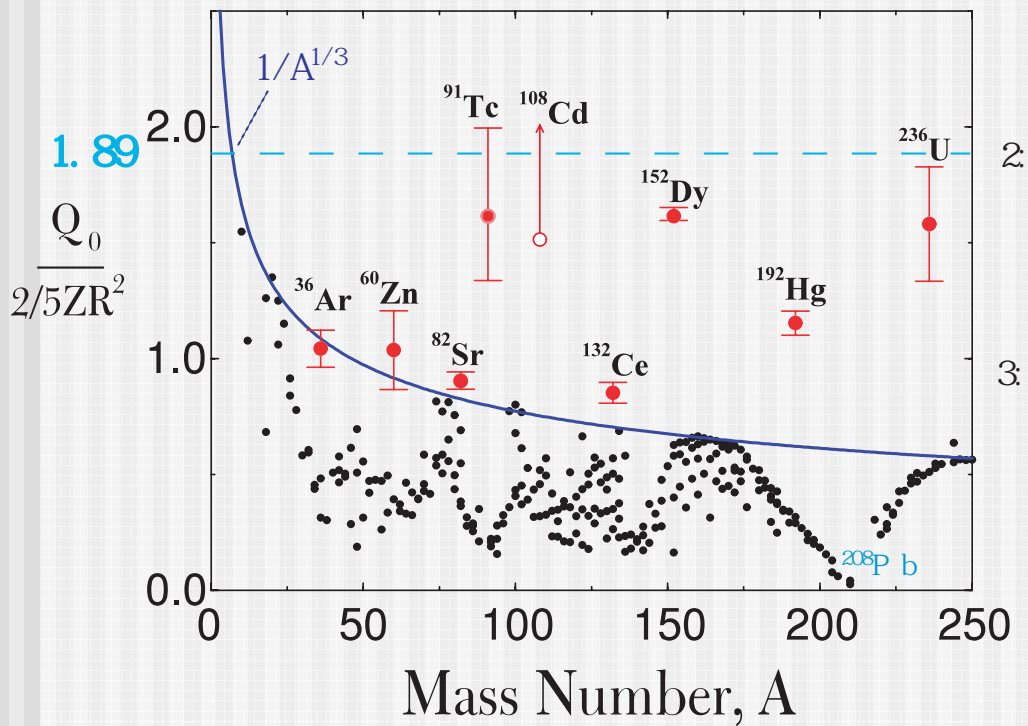
Z First observed in

$^{242}\text{Am}$

SD band in  $^{152}\text{Dy}$   
in 1986



# Limit of deformation



$$Q_0 = \frac{2}{5} Z R^2 \frac{x^2 - 1}{x^{2/3}} \times 10^{-2} eb$$

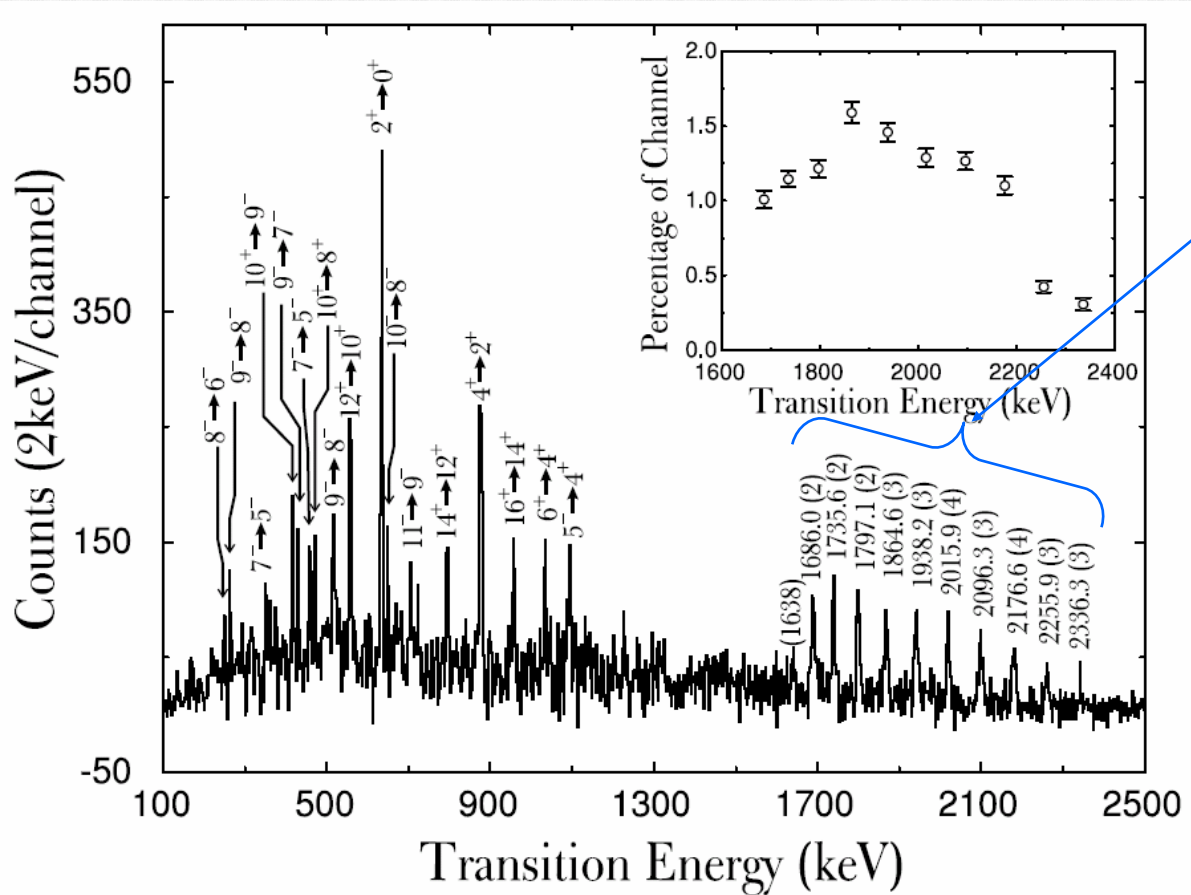
$x$  : major-to-minor  
axis ratio

$x = 2 \rightarrow 2:1$  deformation

$$\frac{Q_0}{2/5 Z R^2} = 1.89$$

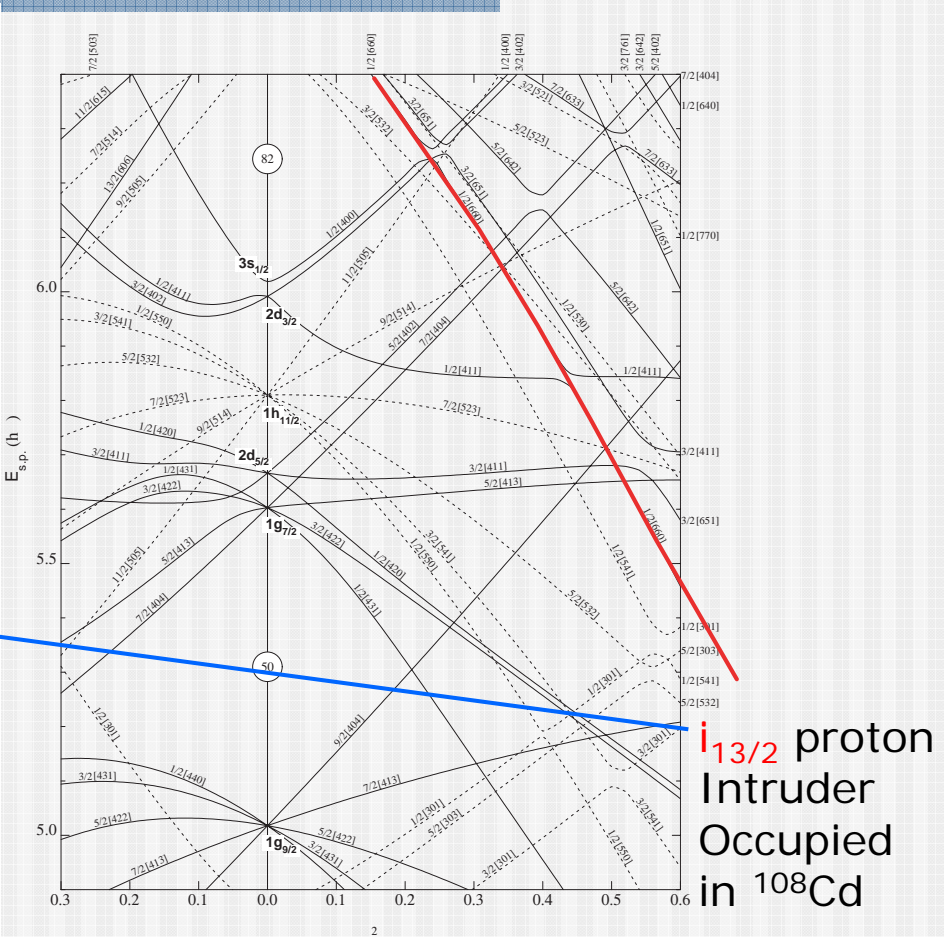
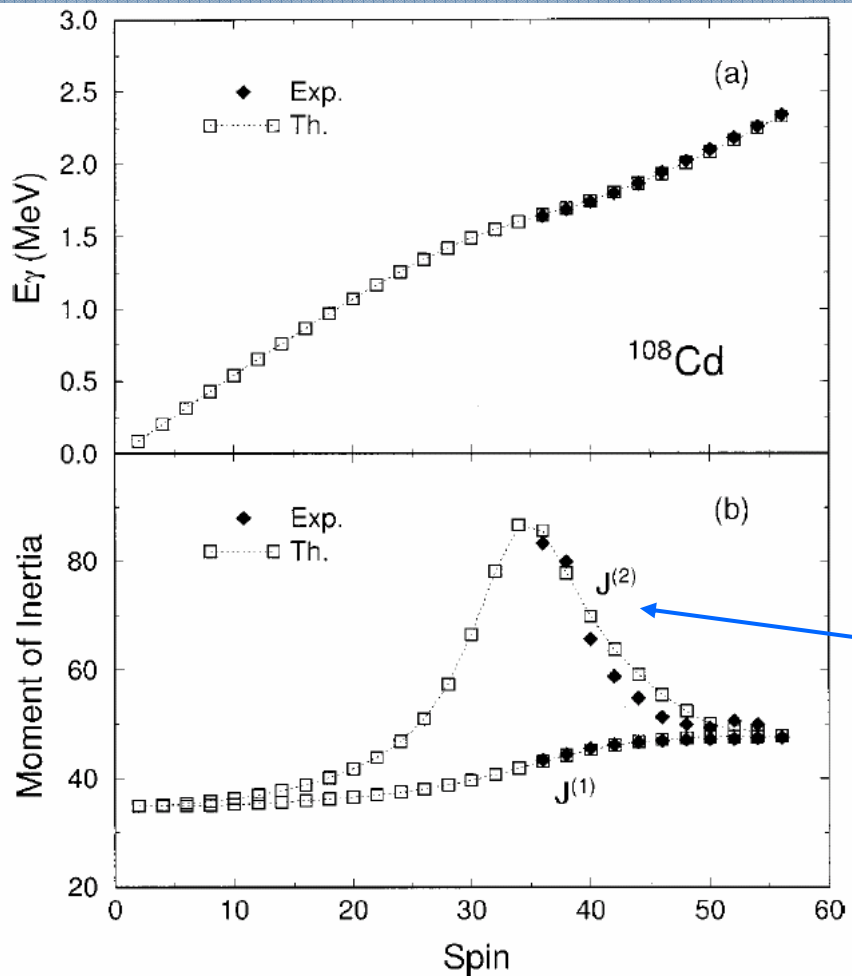
$$R = 1.2 A^{1/3} \text{ fm}$$

# SD band in $^{108}\text{Cd}$



$^{64}\text{Ni}(^{48}\text{Ca},4\text{n})^{108}\text{Cd}$   
207MeV  
@ ATLAS, GS  
ANL

# $i_{13/2}$ intruder orbital

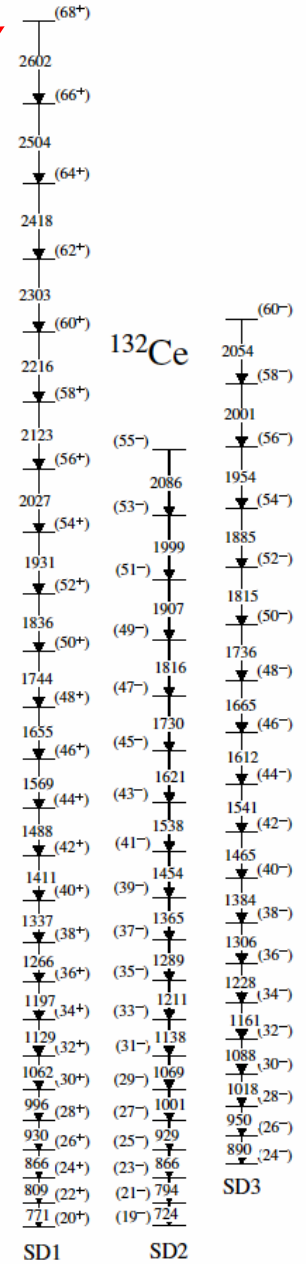
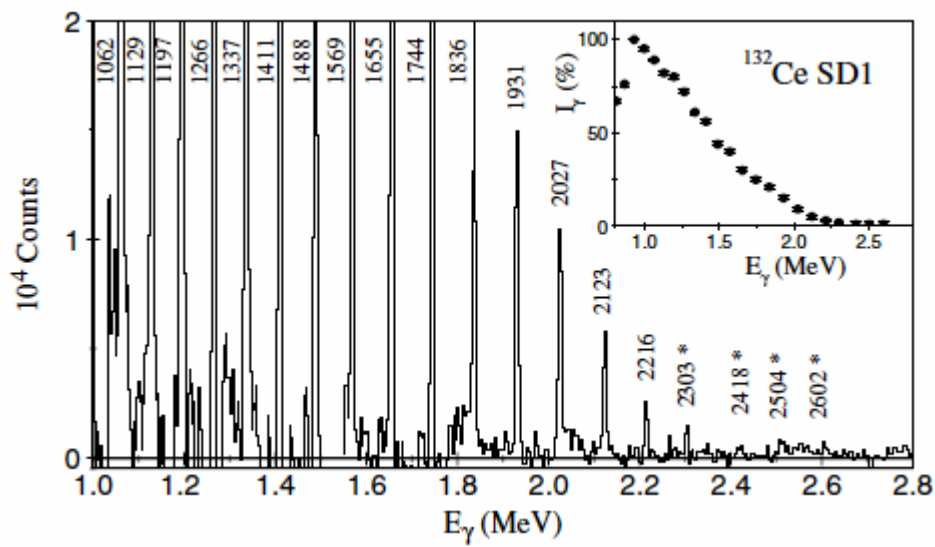


# Highest spin observed

## ■ Superdeformed band in $^{132}\text{Ce}$

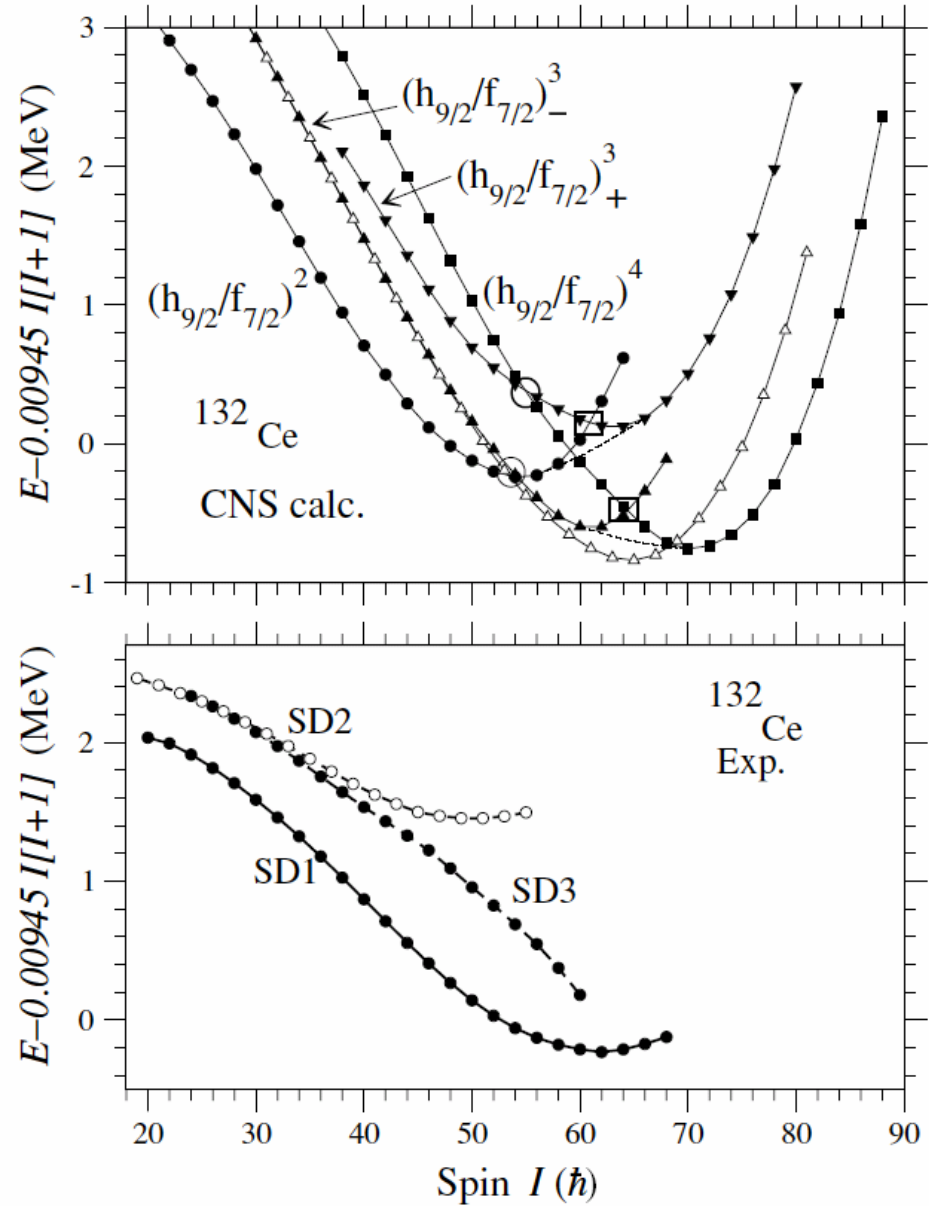
E.S.Paul et al., Phys. Rev. C71, 054309 (2005)

$$I_{\max} = (68+)$$



# Excitation energy

- Excitation energy  
Relative to a rigid Rotor reference
- Comparison with Cranked Nilsson Strutinsky calculation
- Similar behavior with smooth band termination in  $A \approx 110$



# Limit of high-spin

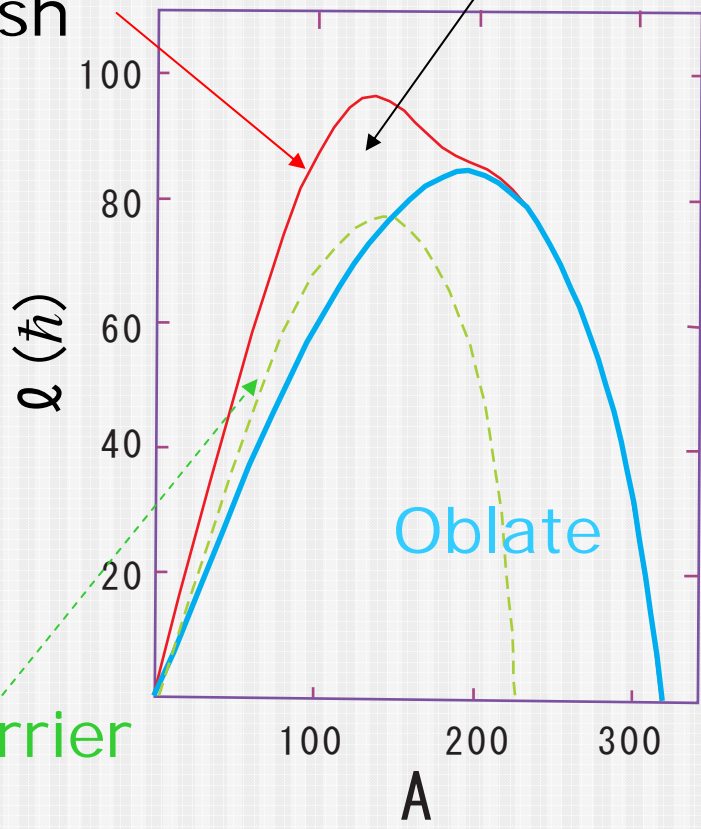
Rotating Liquid Drop  
S. Cohen et al.,  
Ann. Phys. 82, 557 (1974)

- The nuclei able to support the highest angular momenta near  $A \approx 130$
- Fission barrier vanishes at  $97\hbar$

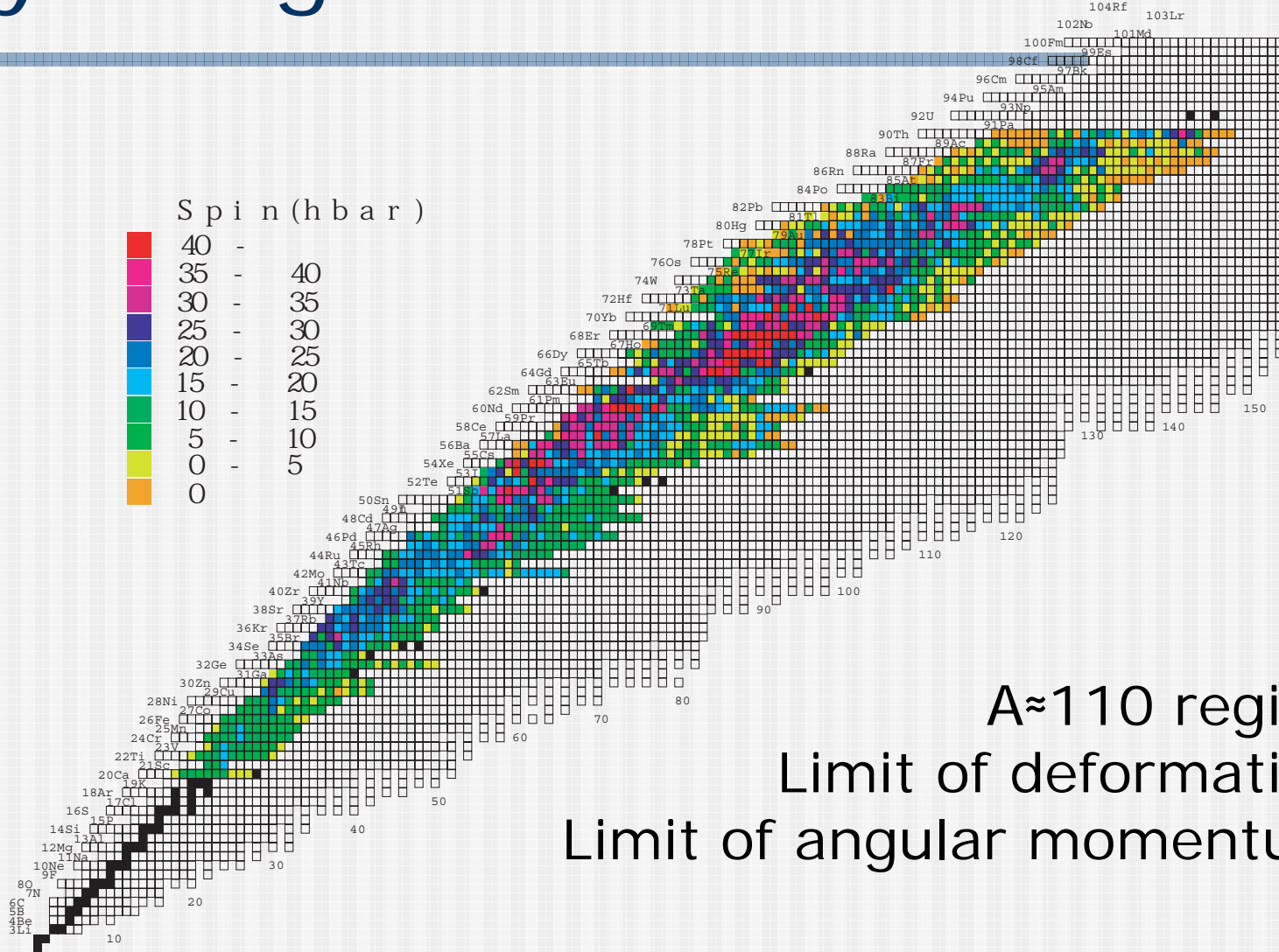
Fission barrier  
 $> 8\text{MeV}$

Fission barrier vanish

Triaxial



# High-spin nuclei studied by using stable nuclear beams



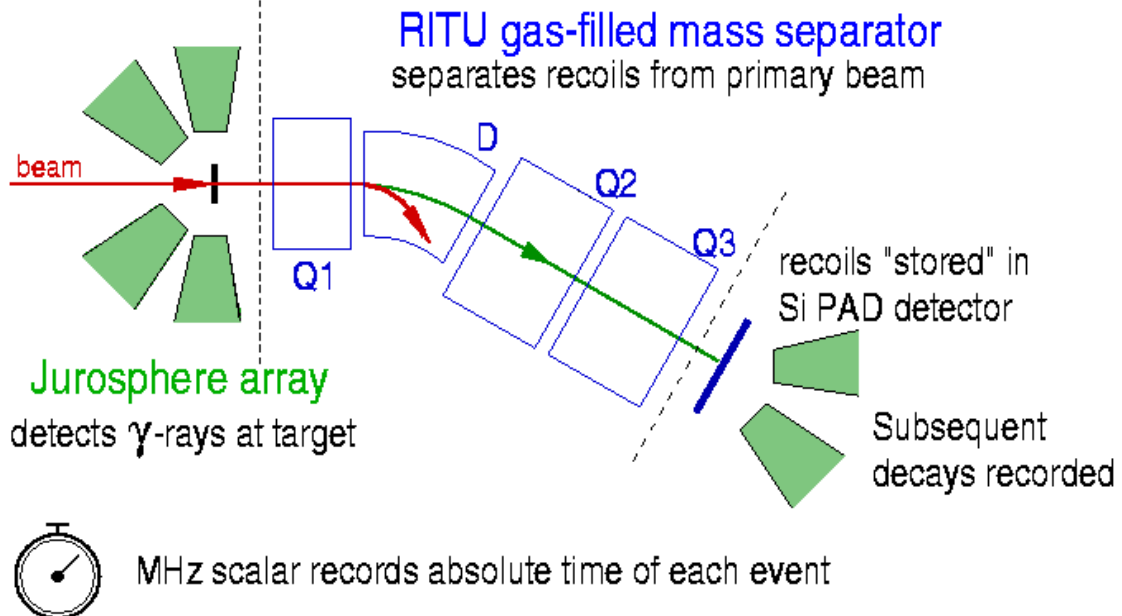
# High-spin studies in proton-rich nuclei

---

- Nuclei produced by fusion-evaporation reaction are in proton rich side relative to the line of  $\beta$ -stability
- By using most proton rich stable beam and target, we can access to the proton rich region
- Proton rich nuclei close to proton drip line often decay by  $\alpha$  decay or proton decay  
→ using **tagging technique** to access proton rich limit (Jyväskylä, ANL)
- Many proton rich nuclei can also be studied ( $^{107}\text{In}$ )

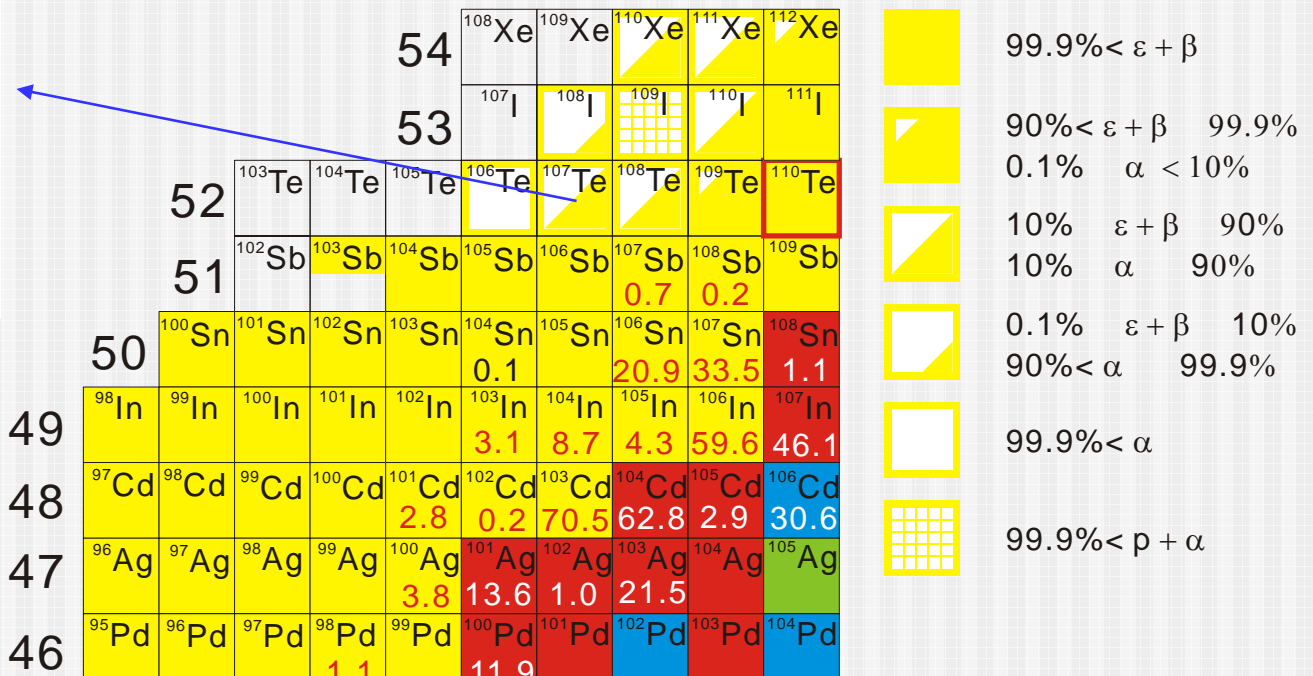
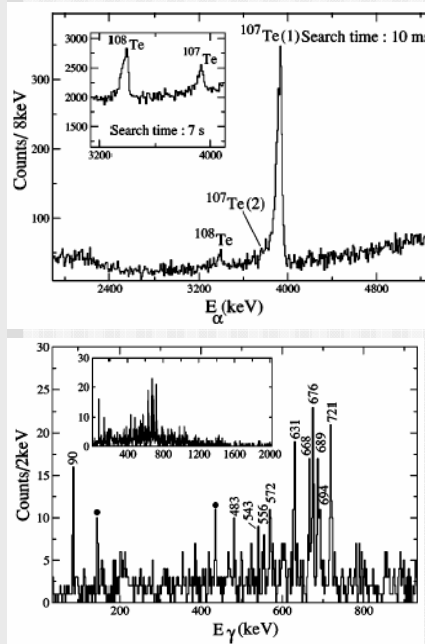
# Recoil decay tagging

## Correlated radioactive decay - apparatus



# Study of $^{107}\text{In}$ (Z=49, N=58)

Reaction :  $^{52}\text{Cr}(187\text{MeV}) + ^{58}\text{Ni}(580+640 \mu\text{g/cm}^2)$



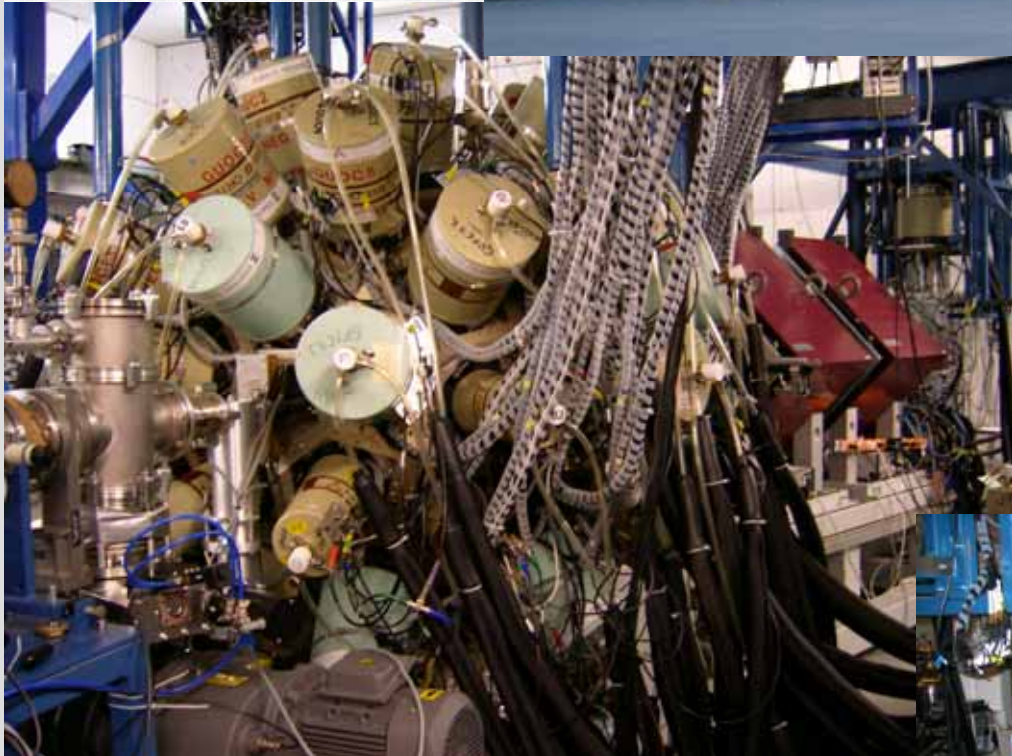
B. Hadinia et al.  
PRC70, 064314(2004)

$^{58}\text{Ni}(^{52}\text{Cr}, 3p)^{107}\text{In}$

# Experimental Setup

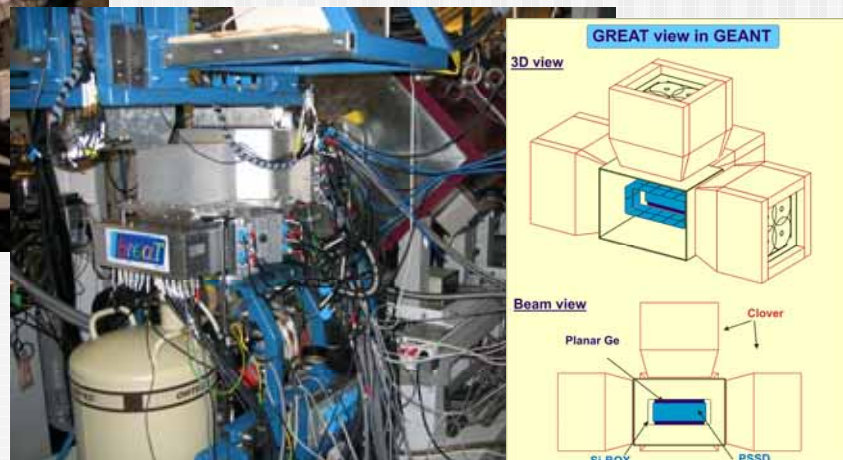


University of Jyväskylä

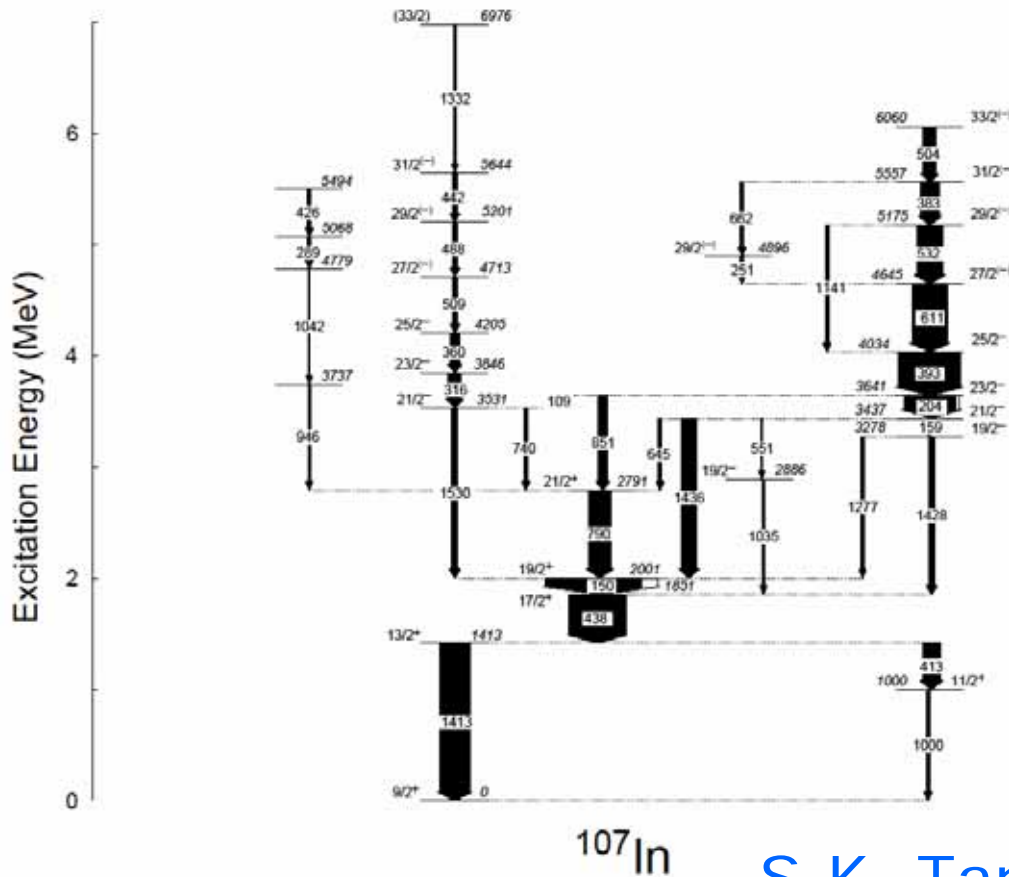


JUROGAM  
43 Ge + BGO  
+ RITU  
Gas filled Ion Sep.  
+ GREAT spectrometer

GREAT:  
Double sided Si strip  
Si PIN photodiode array  
Double sided planar Ge  
Segmented Clover Ge

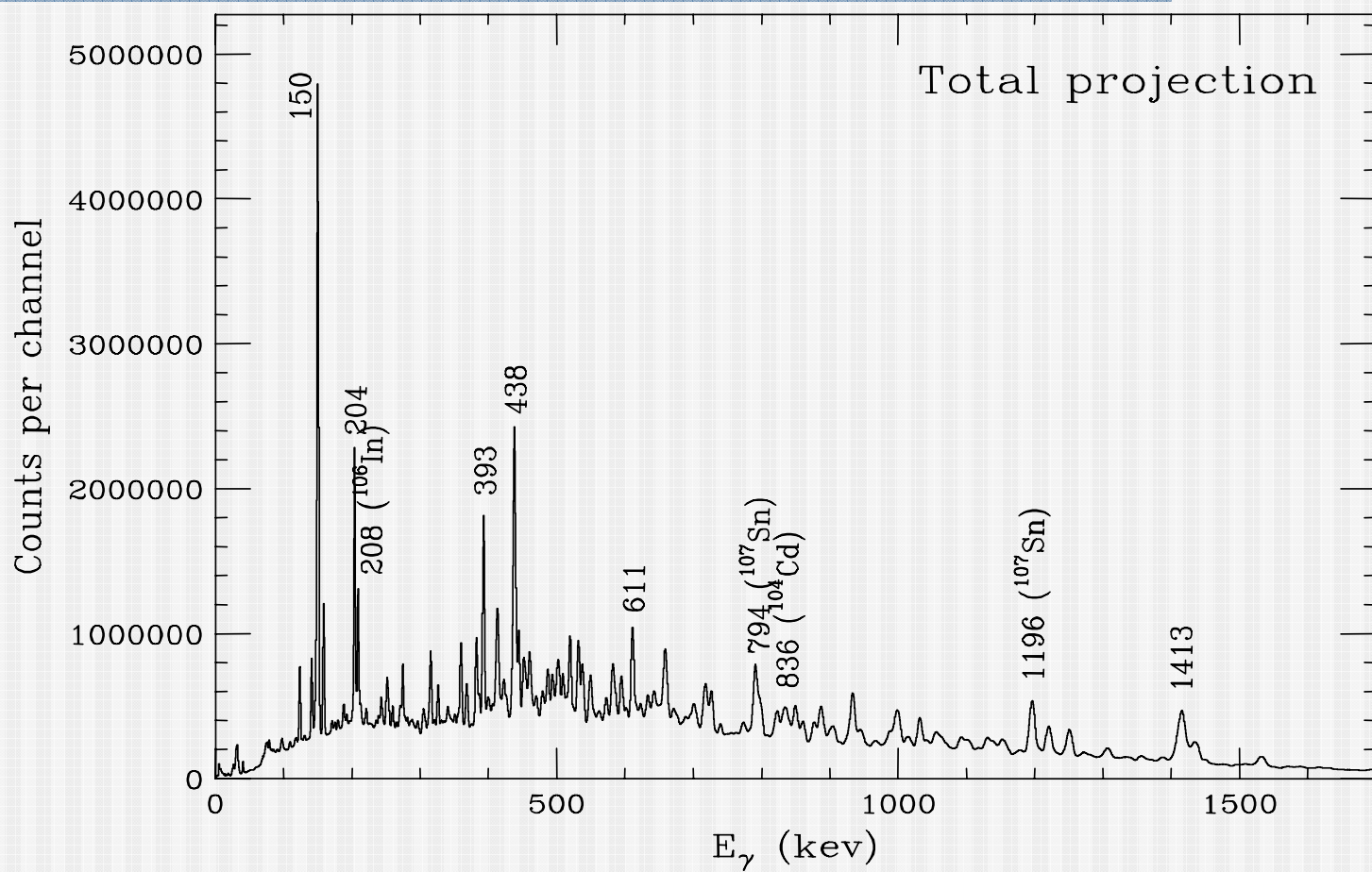


# $^{107}\text{In}$ level scheme

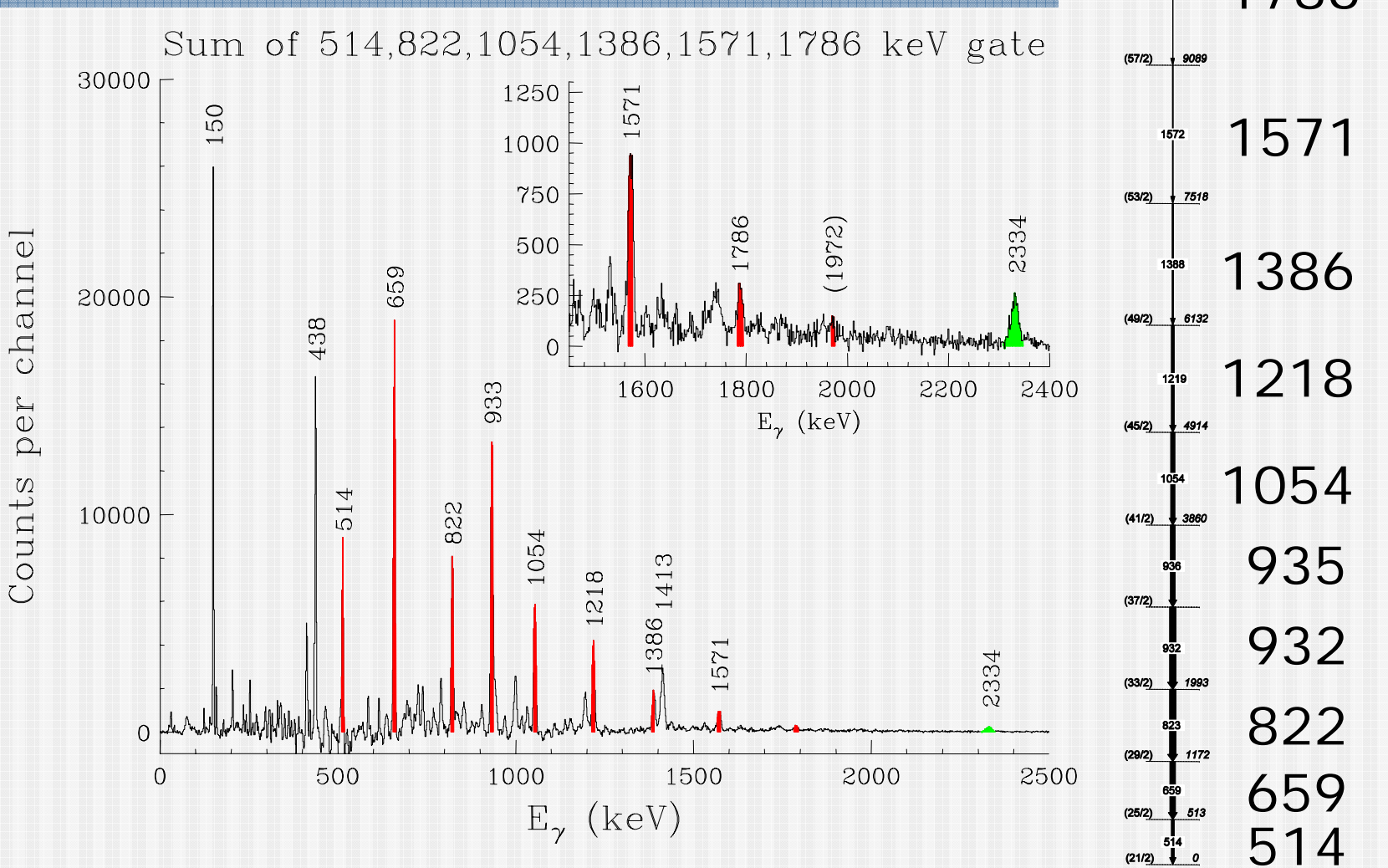


S.K. Tandel et al.  
PRC58, 3738 (1998)

# Gamma-ray spectrum

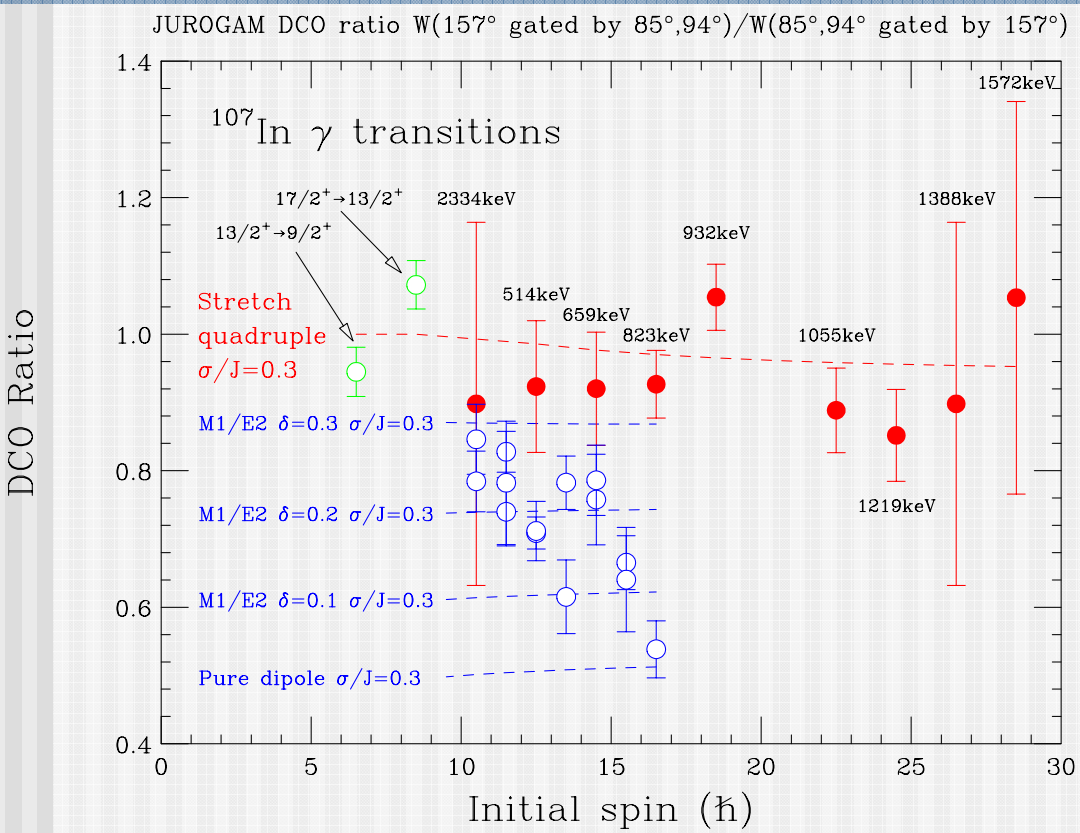


# A rotational band in $^{107}\text{In}$



# DCO ratio analysis

(Directional Correlation from Oriented nuclei)

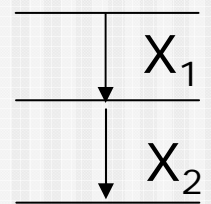


DCO Ratio:

$$R = \frac{W(\theta_1, \theta_2, \phi)}{W(\theta_2, \theta_1, \phi)}$$

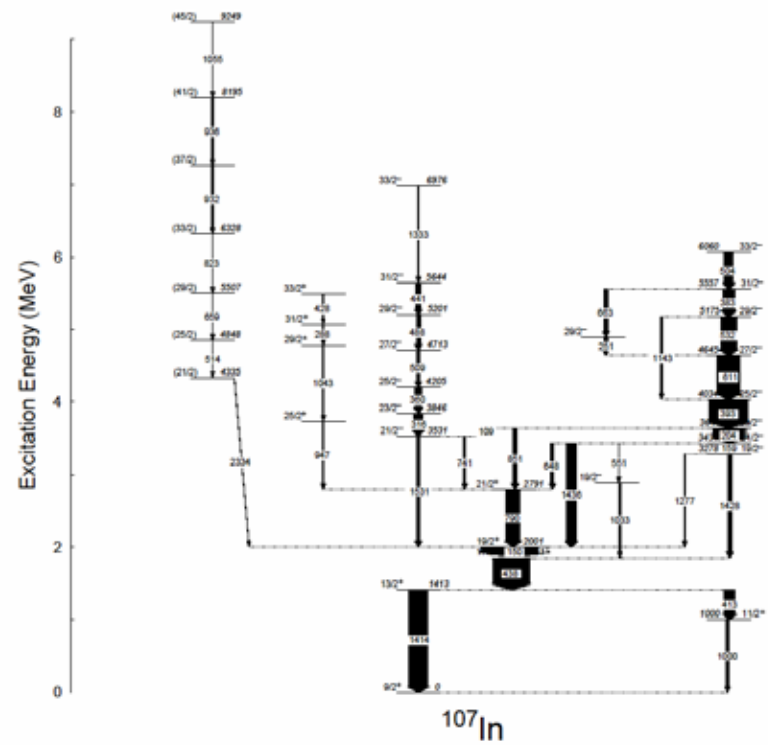
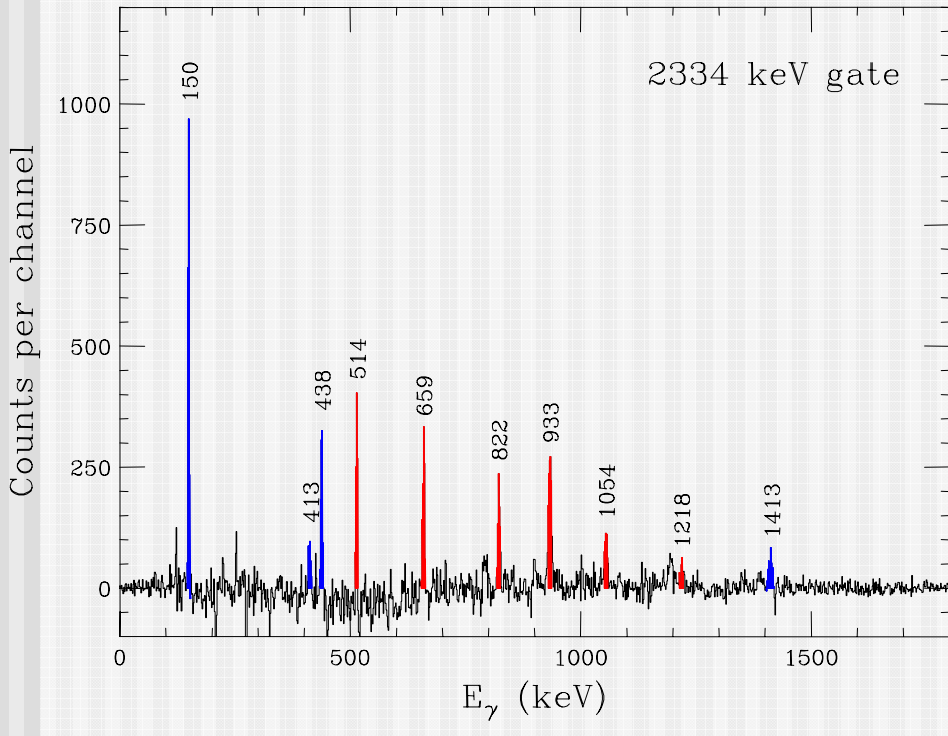
Consistent with E2  
of in-band transition  
Most of known transitions  
are dipole | Mixed

$\sigma/J$  : alignment parameter  
 $\sigma=0$  : complete alignment  
 $\delta$  : mixing ratio



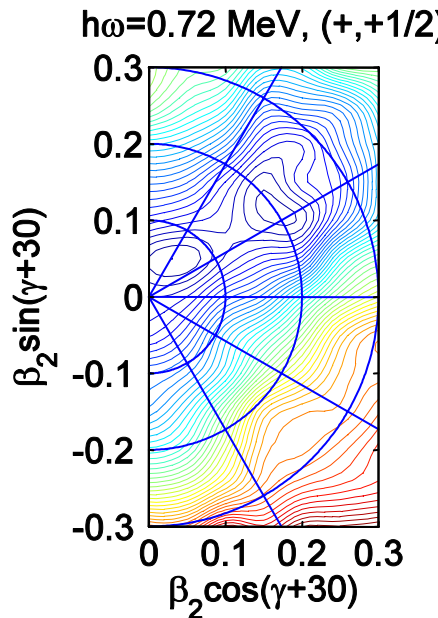
$$W(\theta_1, \theta_2, \phi) = N \sum_{\lambda\lambda_1\lambda_2} B_{\lambda_1}(I_1) A_{\lambda}^{\lambda_2\lambda_1}(X_1) A_{\lambda_2}(X_2) H_{\lambda_1\lambda\lambda_2}(\theta_1, \theta_2, \phi)$$

# Linking transition

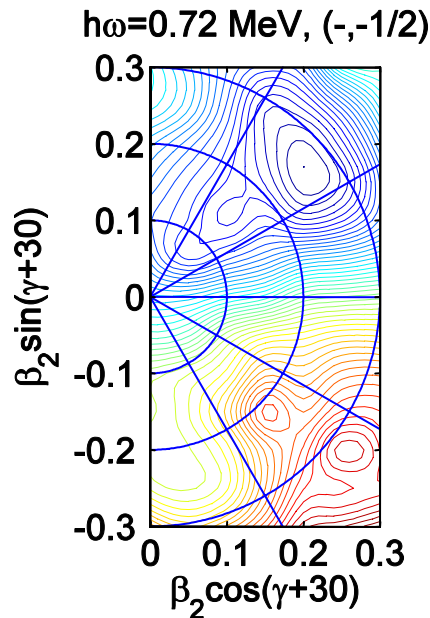


# Total Routhian Surface (TRS) Calculation

A conf.

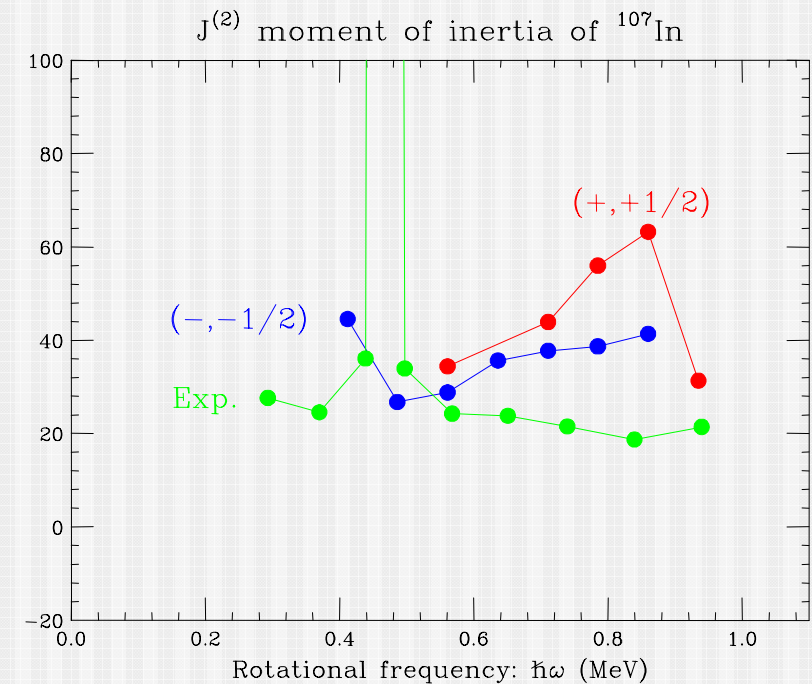
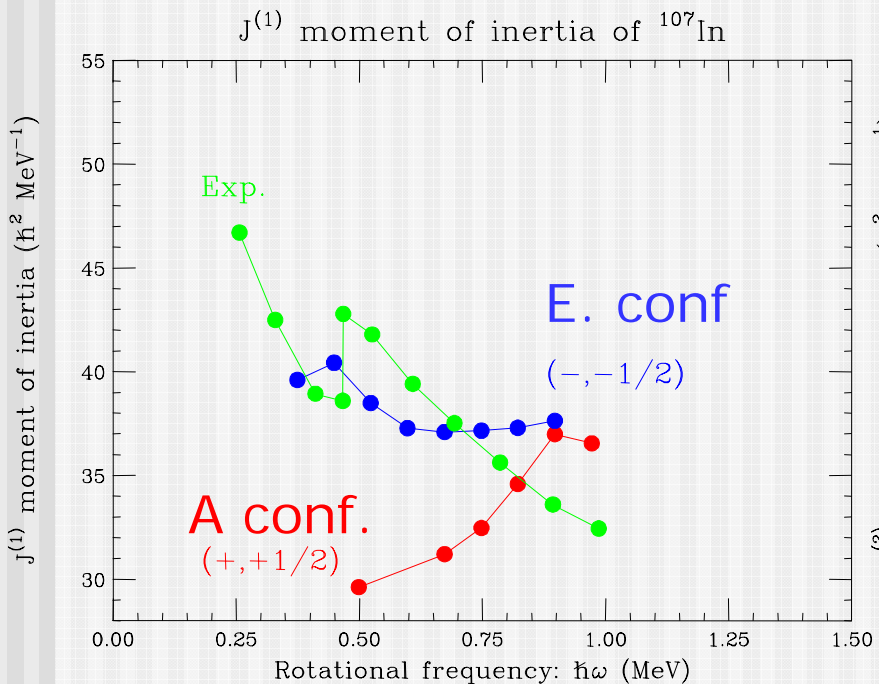


E. conf.



Deformed minima with  $\beta_2 \sim 0.2 - 0.3$

# $J^{(1)}, J^{(2)}$ moment of inertia Exp. and TRS calc.



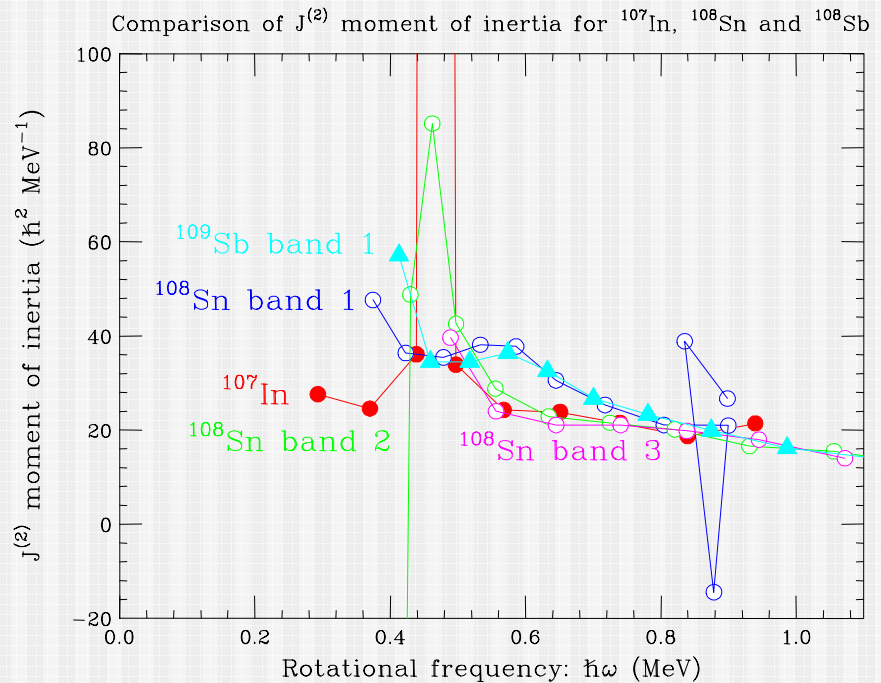
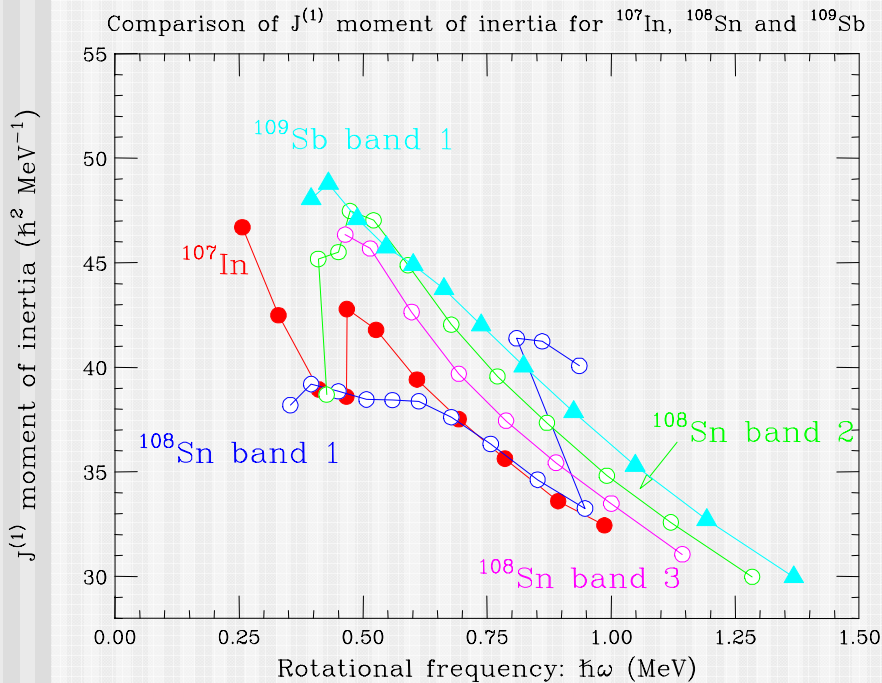
Kinematical

$$J^{(1)} = \left[ \frac{2}{\hbar^2} \frac{dE(I)}{d(I^2)} \right]^{-1} = \hbar \frac{I}{\omega}$$

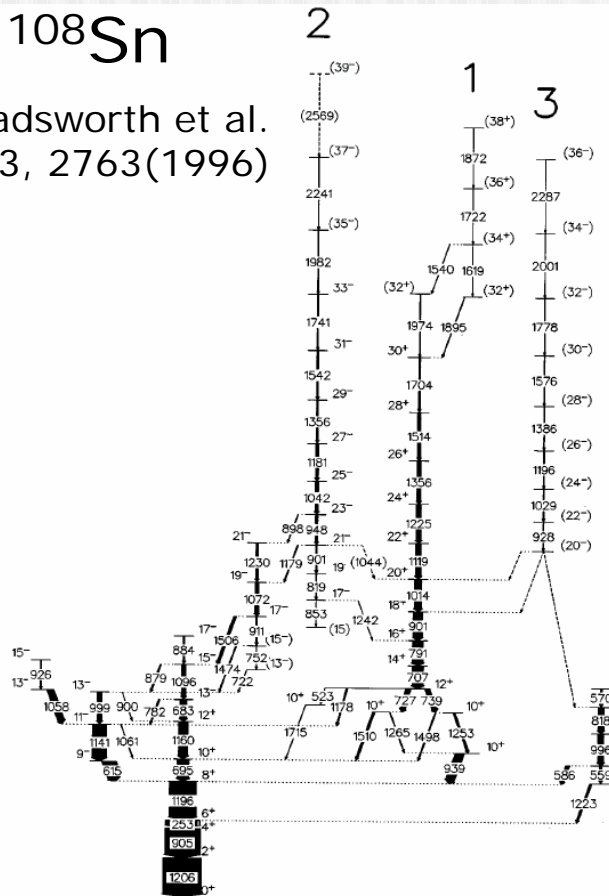
Dynamical

$$J^{(2)} = \left[ \frac{1}{\hbar^2} \frac{d^2E(I)}{dI^2} \right]^{-1} = \hbar \frac{dI}{d\omega}$$

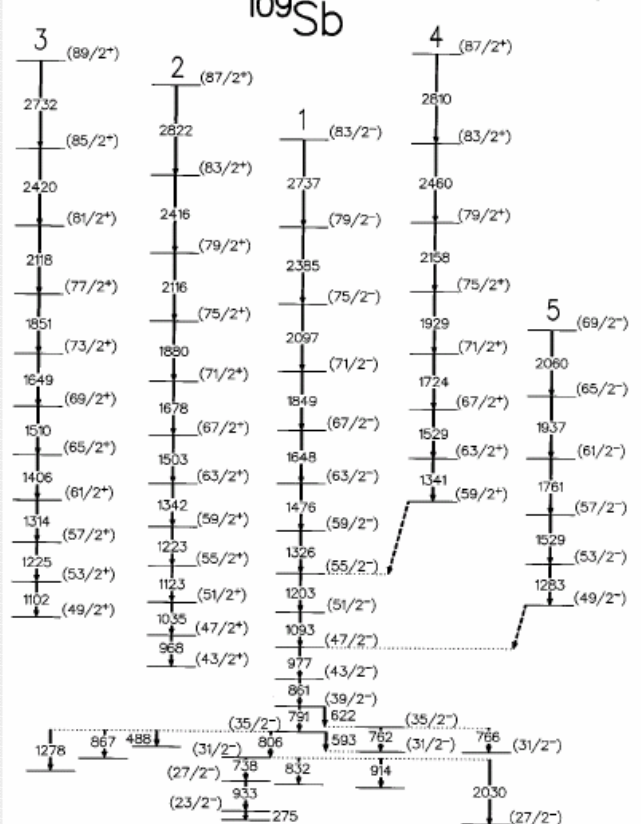
# $J^{(1)}$ and $J^{(2)}$ moment of inertia



# Smooth band termination in A~110 region



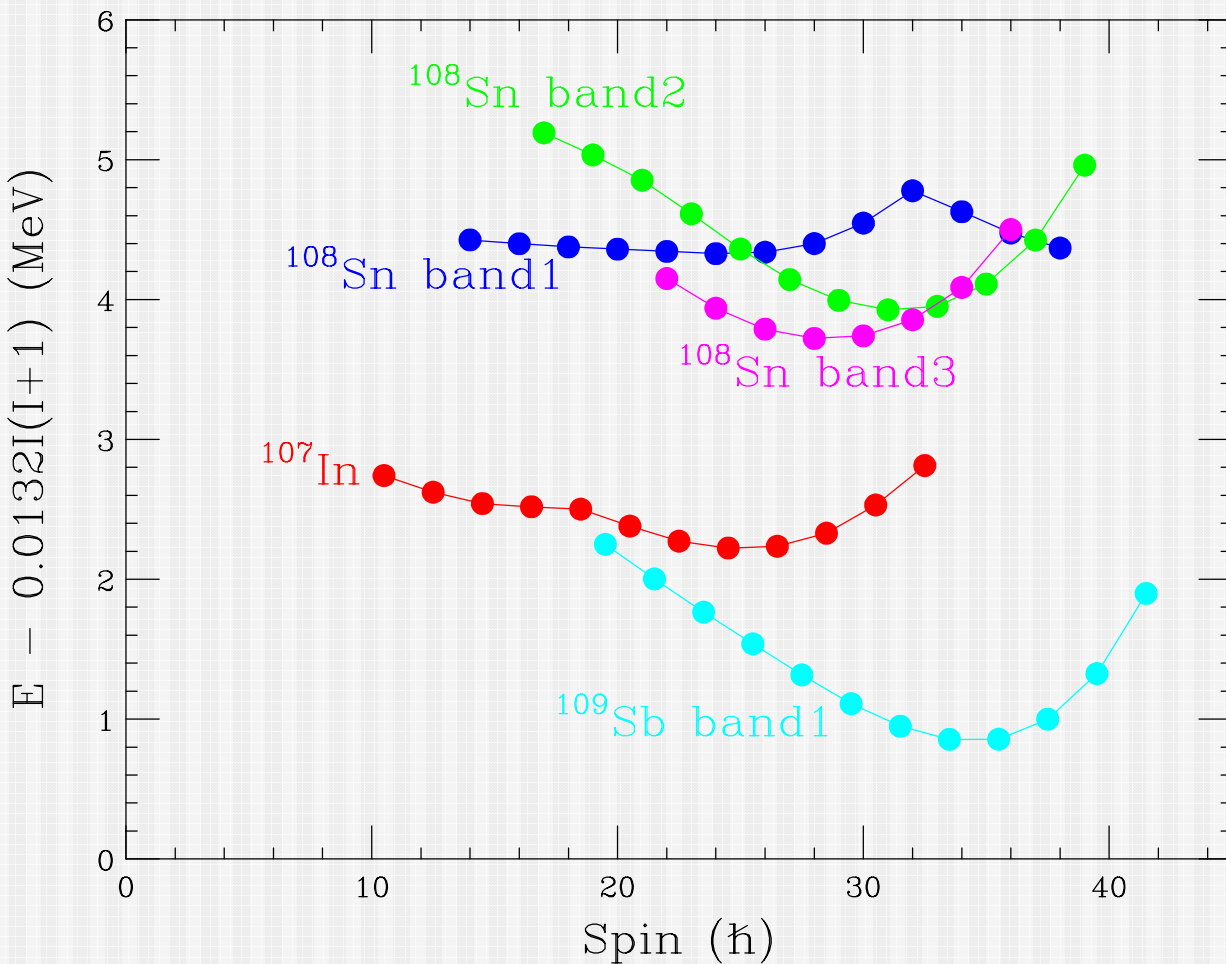
$^{109}\text{Sb}$   
H. Schnare et al.  
PRC54, 1598(1996)



$\pi[g_{9/2}^{-2}(g_{7/2}h_{11/2})] \otimes v[(d_{5/2}g_{7/2})^6h_{11/2}^2]$   
terminate@39-

$\pi[g_{9/2}^{-2}(g_{7/2}d_{5/2})h_{11/2}] \otimes v[(d_{5/2}g_{7/2})^6h_{11/2}^2]$   
terminate@83/2-

# Excitation energy relative to rigid rotor reference



# High-spin study in neutron rich nuclei

---

Fusion reaction:

- Stable isotope beam + Stable isotope target  
→ High-spin states in proton-rich nuclei

High-spin study induced by RI beam

Fusion reaction:

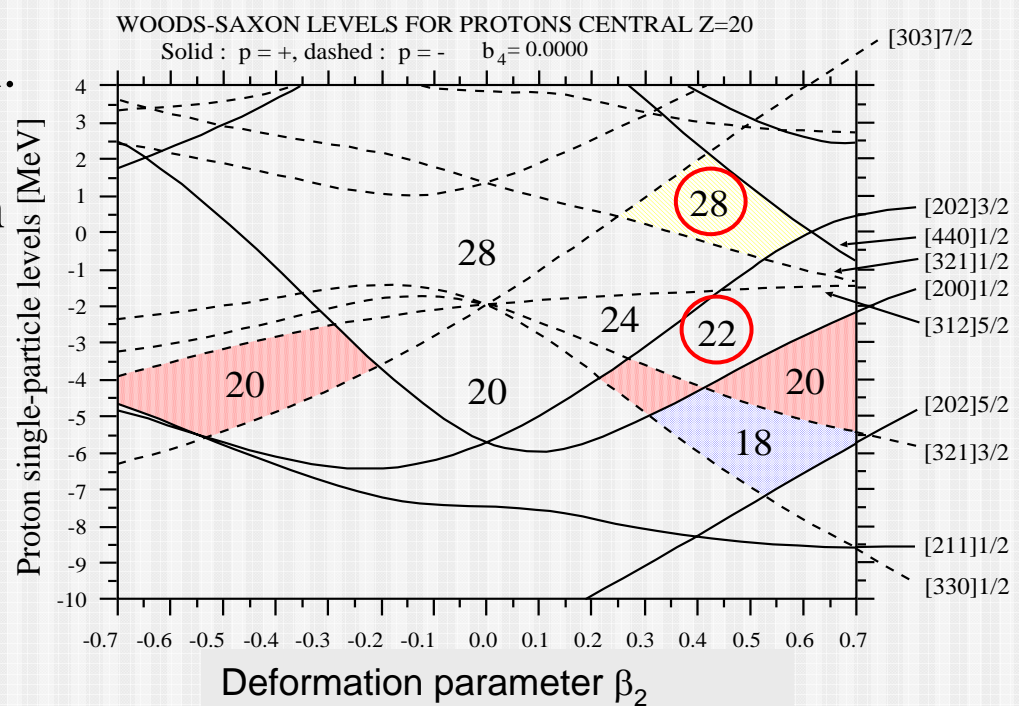
- RI beam** + Stable isotope target  
→ High-spin states in Stable | Neutron-rich nuclei

# Study of $^{49-52}\text{Ti}$ ( $Z=22, N=27-30$ )

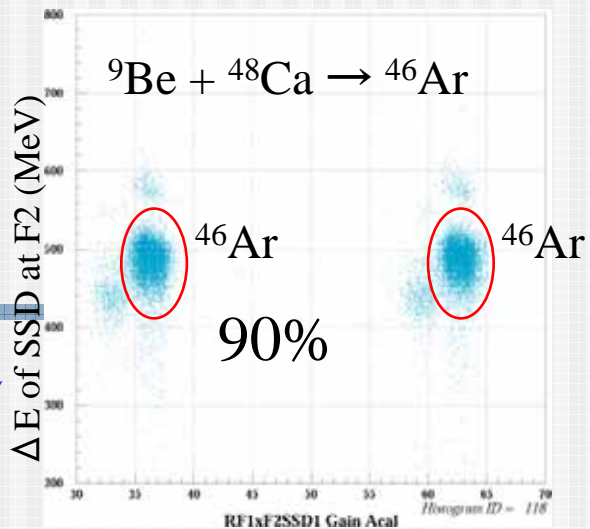
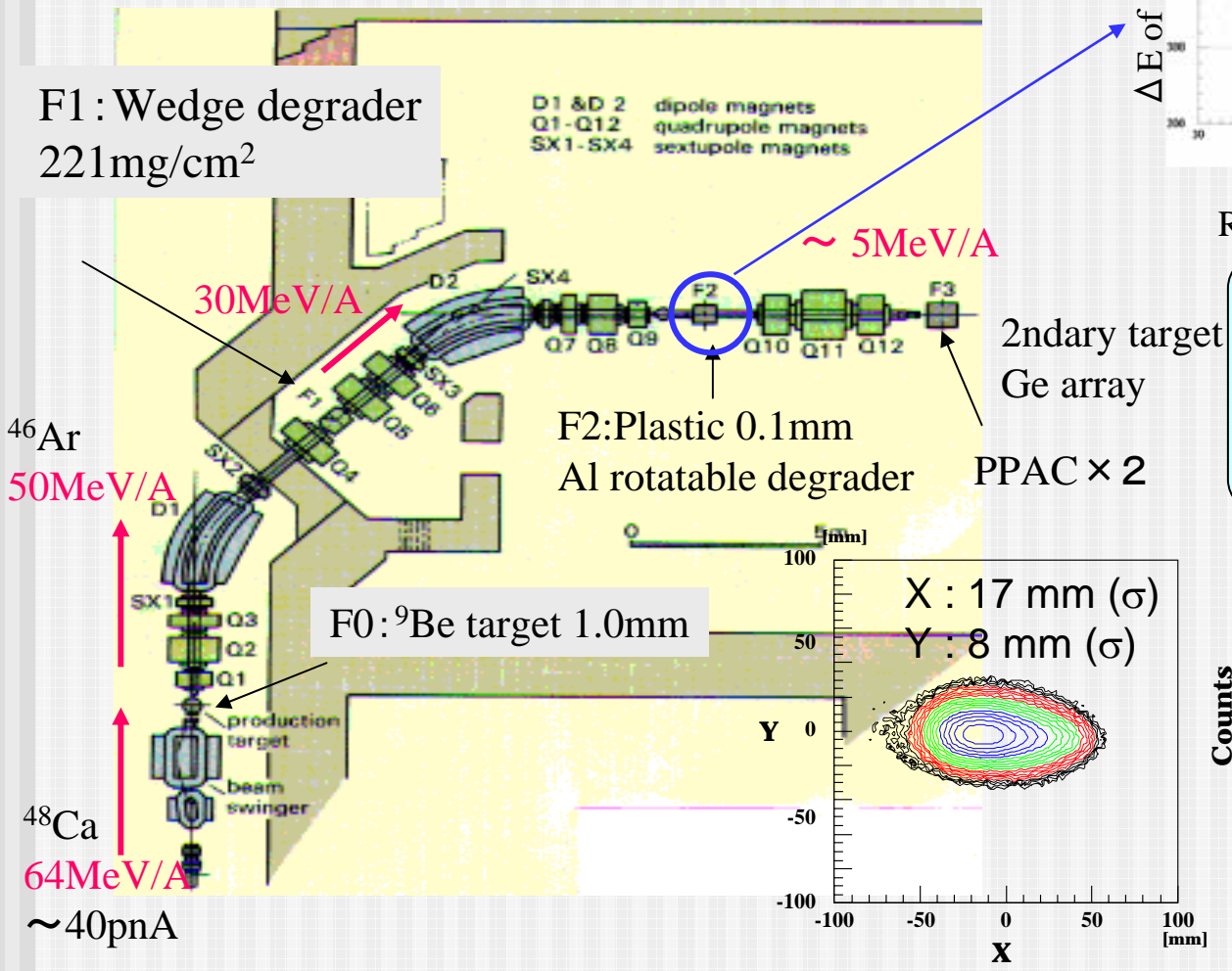
High-spin study of  
most neutron-rich stable nuclei.  
→  $^{48}\text{Ca}$  and neighbors  
deformed states at high spin

$^{50}\text{Ti}$  ( $Z=22, N=28$ )

→ Deformed collective band  
at high-spin

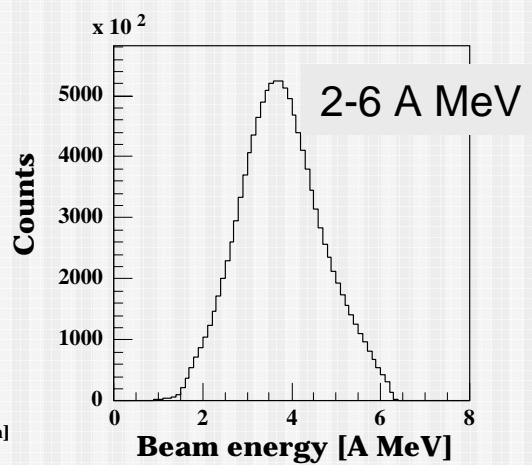
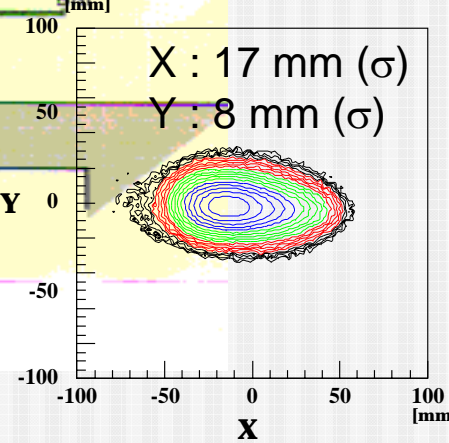


# Low-energy 2ndary beams using RIPS



RF - F2 Plastic TOF (ns)

$^{46}\text{Ar}$  beam intensity  
 $F2 : 7.3 \times 10^5 \text{ cps}$   
 $F3 : 3.2 \times 10^5 \text{ cps}$   
Purity : 90 %



# Setup around 2ndary target

Secondary target :  ${}^9\text{Be}$   $10 \mu\text{m}$  ( $1.8\text{mg/cm}^2$ ) thick,  $10\text{cm}\phi$

## Doppler correction:

2 PPACs before 2ndary target

→ Beam Image, incident angle on target

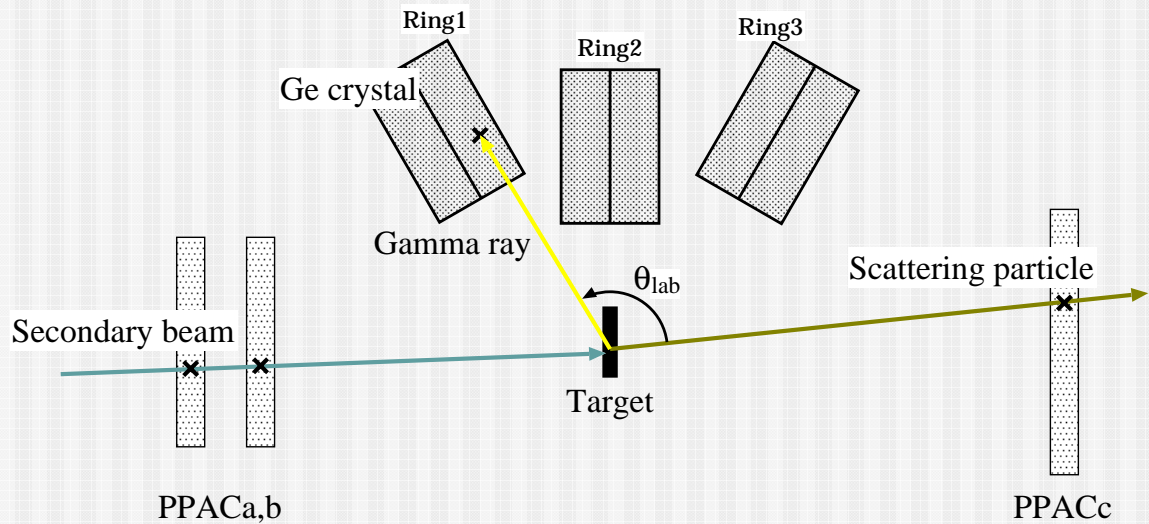
F2 Plastic – F3PPAC TOF

→ Beam Energy

GRAPE(CNS Ge Array, position sensitive)

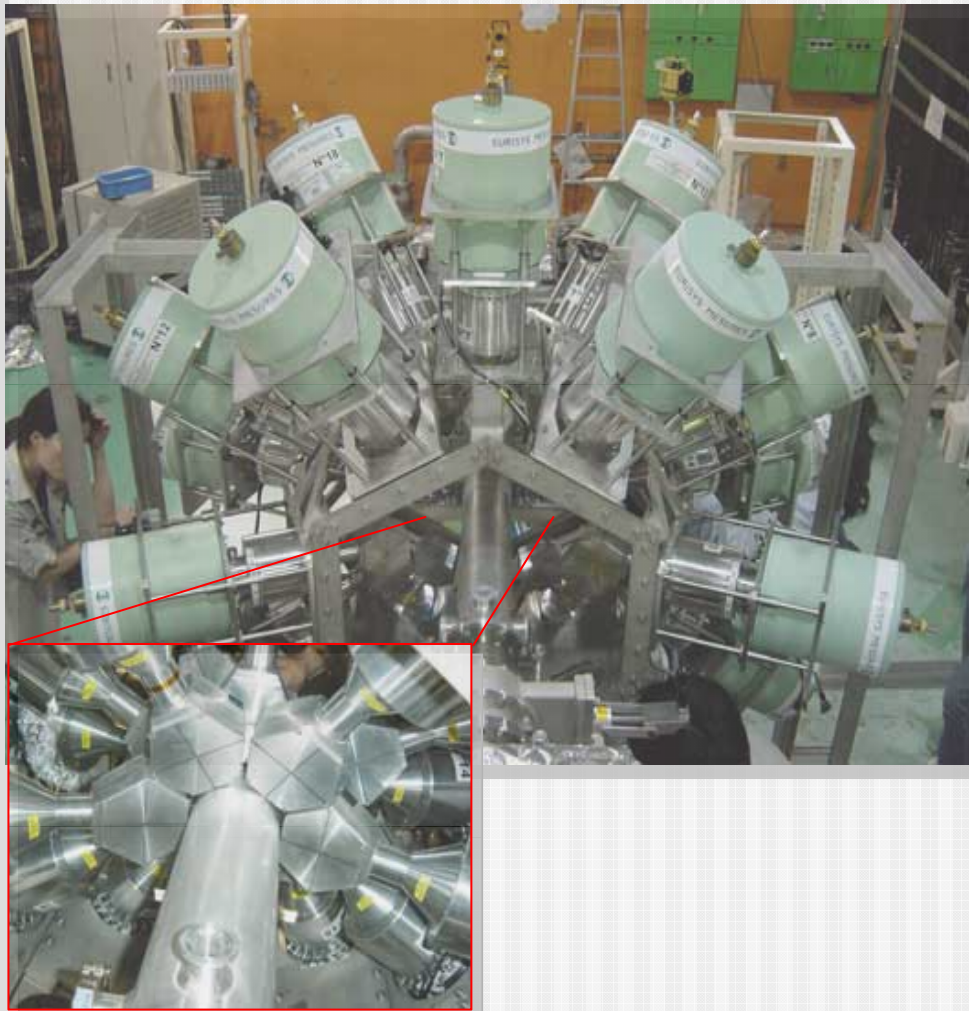


## GRAPE



# GRAPE

(Gamma-Ray detector Array with Position and Energy sensitivity)



18 segmented Ge detectors  
 $\varepsilon \sim 4\%$  for 1MeV  
~ 5mm position sensitivity  
for depth direction

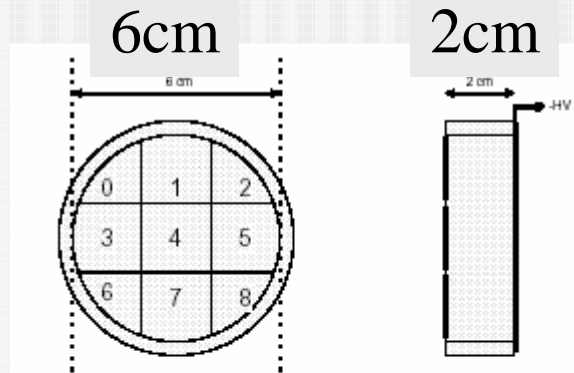
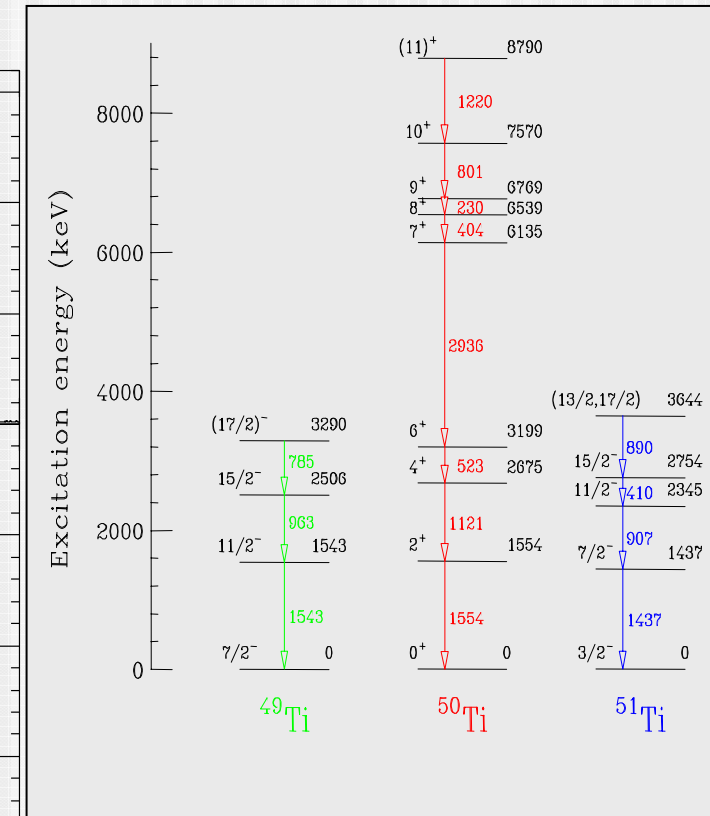
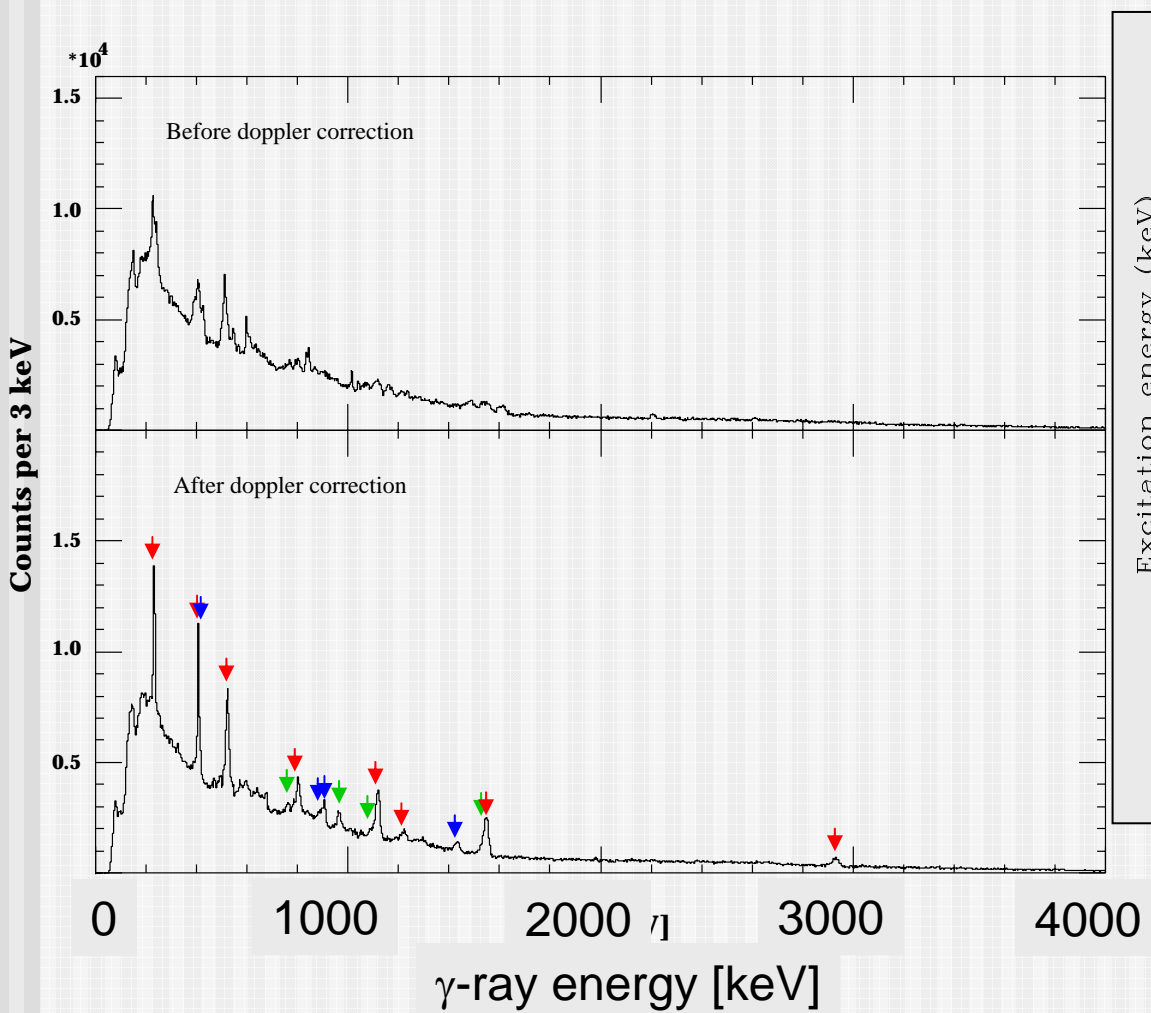


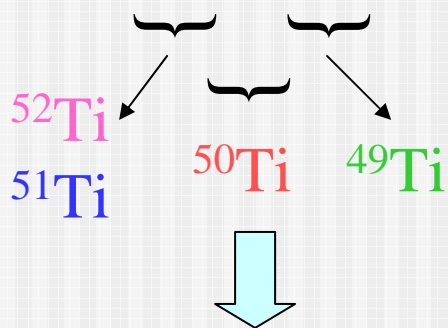
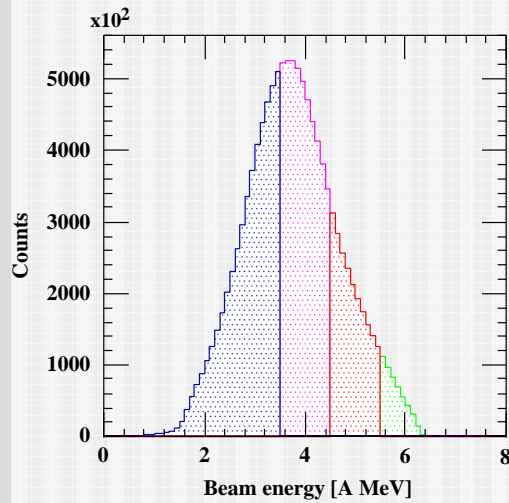
Figure 1: Illustration of a Ge detector.

type	$d$	$\rho$ ( $\text{cm}^{-3}$ )
p <sup>+</sup> (segmented)	0.2 $\mu\text{m}$	$10^{14}$
p	2.0 cm	$0.8 \times 10^{10}$
n <sup>+</sup> (high voltaged)	300 $\mu\text{m}$	$10^{14}$

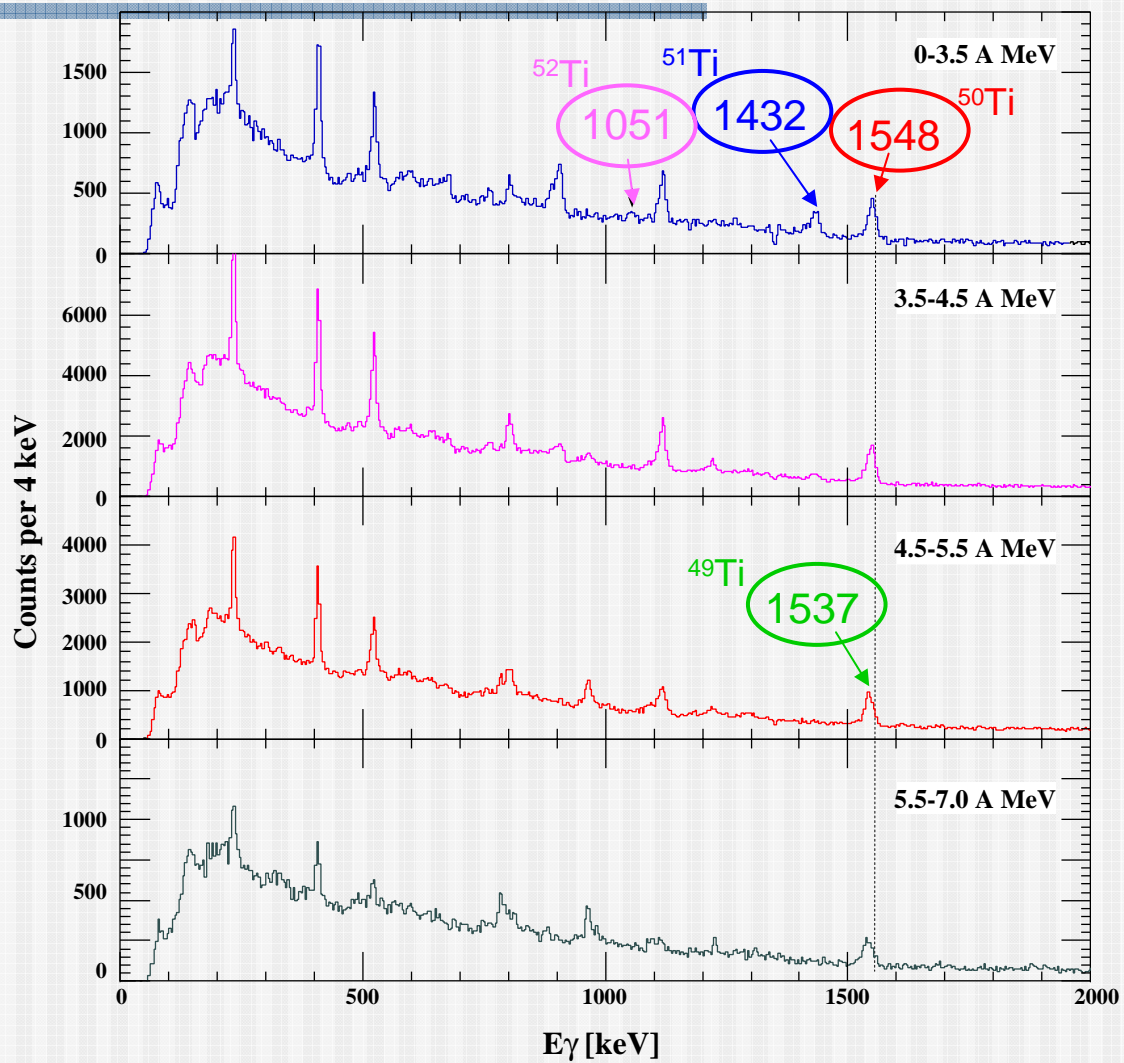
# Gamma-ray spectra in ${}^9\text{Be}({}^{46}\text{Ar}, \text{xn}){}^{55-\text{x}}\text{Ti}$ reaction



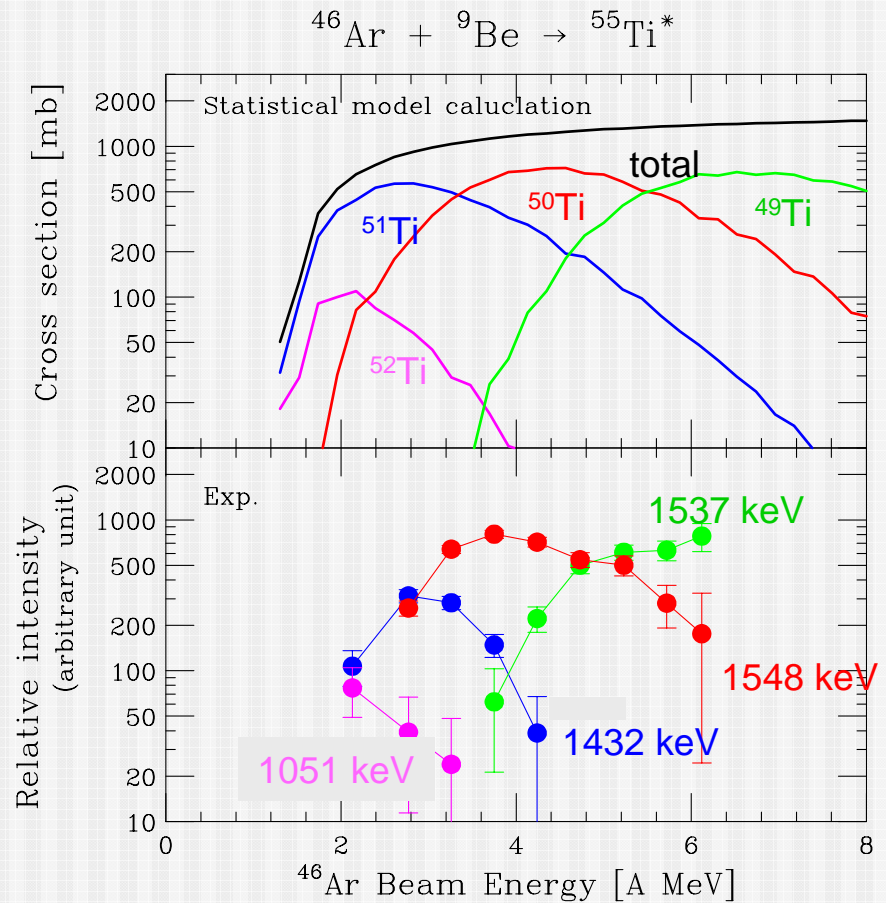
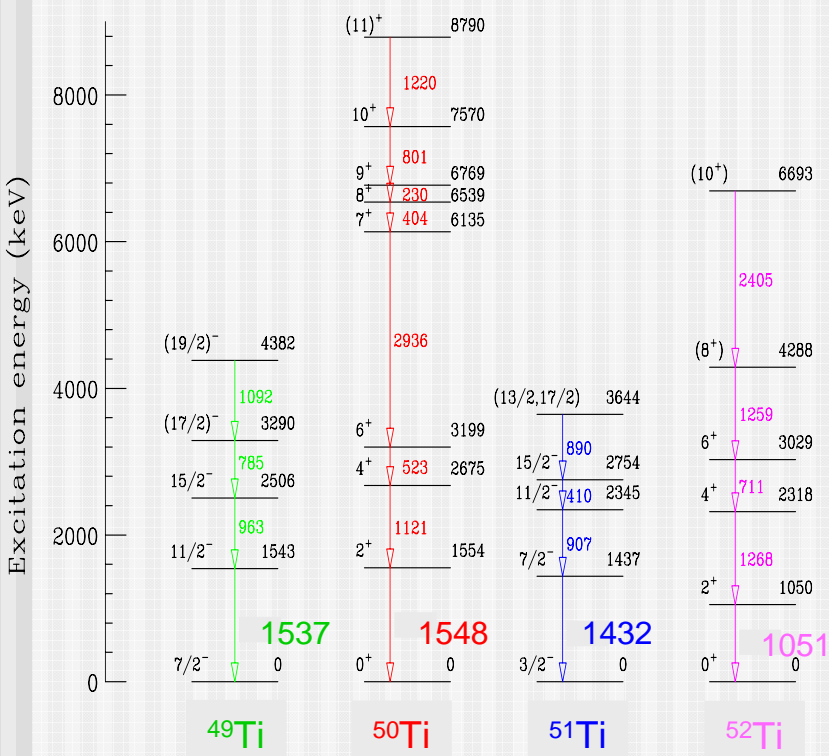
# Excitation function measurements



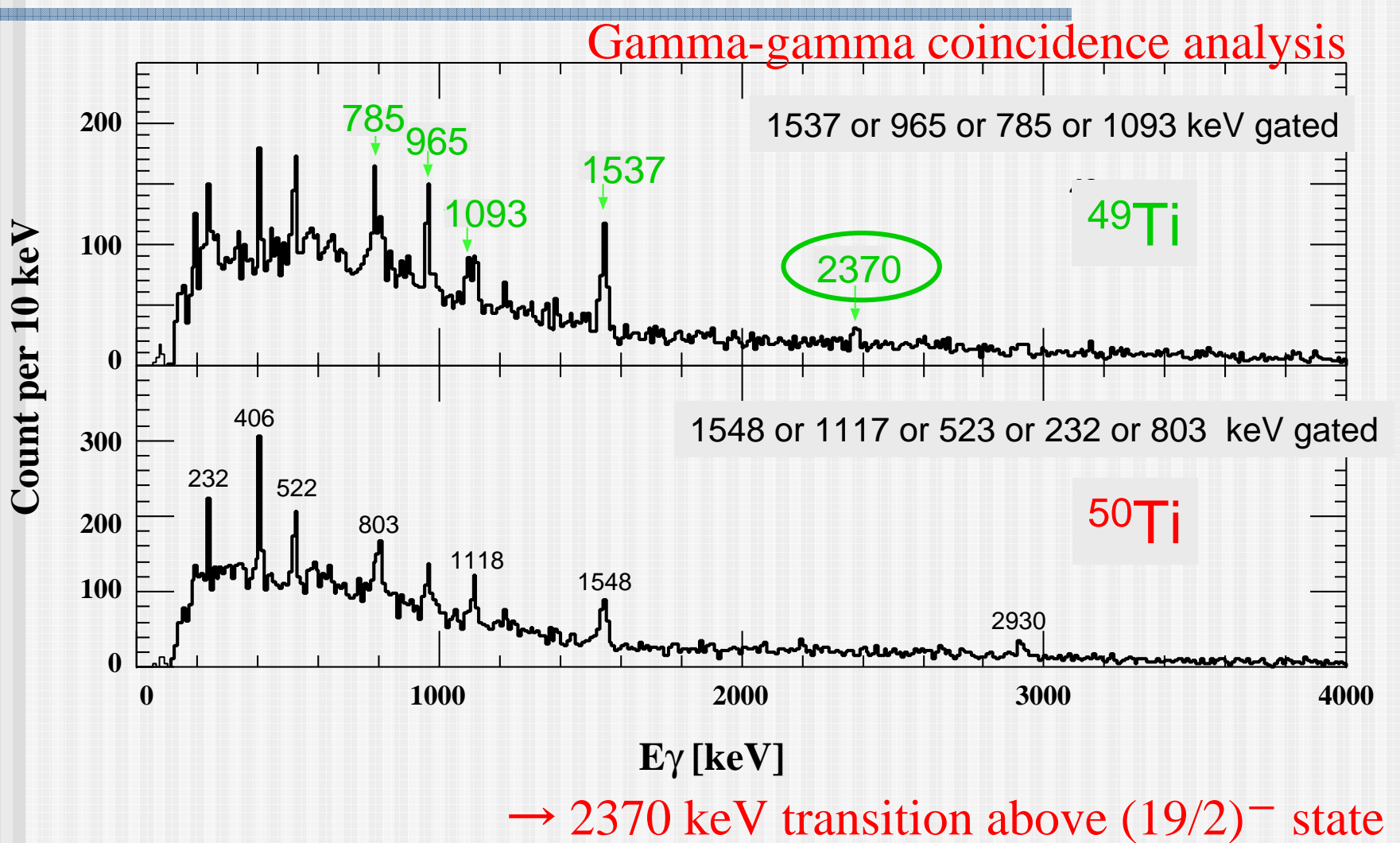
Gamma-ray assignment



# Excitation function

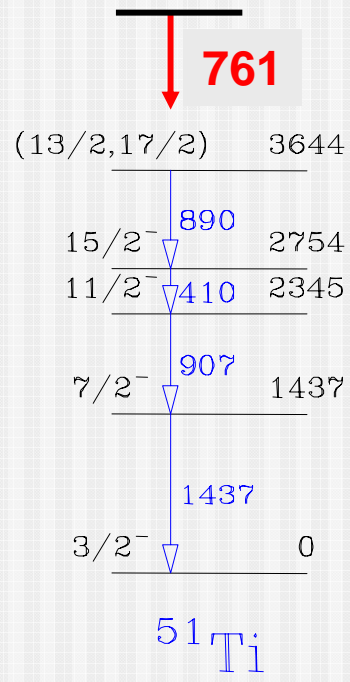
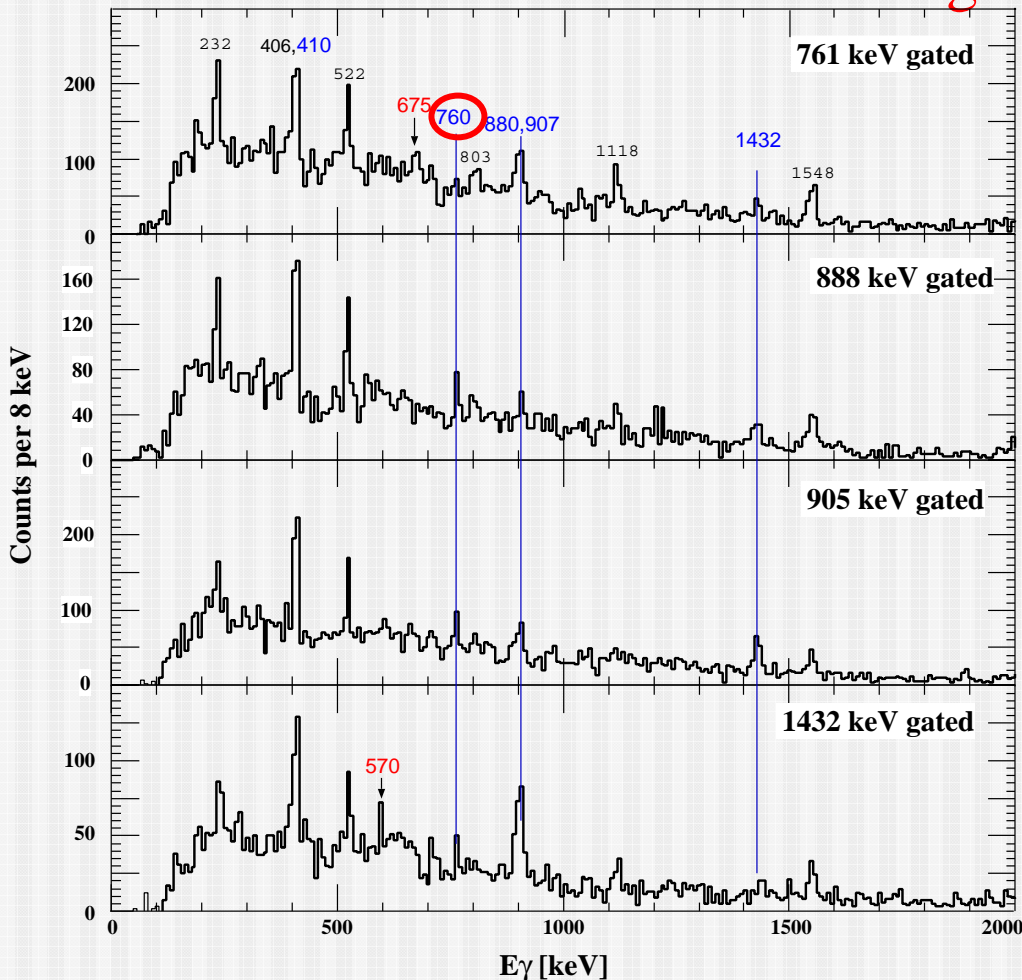


# New transition in $^{49}\text{Ti}$



# New transition in $^{51}\text{Ti}$

Gamma-gamma coincidence analysis



761 keV transition  
above (13/2, 17/2) state

# Future prospects

At present facility with RI-beam

- Fusion reaction of RI beams for high-spin study

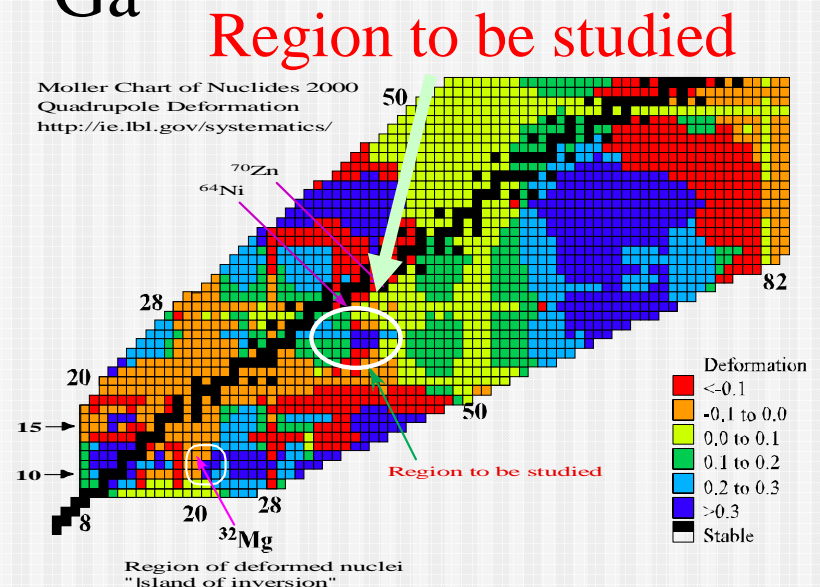
$^{44}\text{S}$  beam  $\rightarrow {}^9\text{Be}(^{44}\text{S}, \text{xn}) {}^{53-\text{x}}\text{Ca}$

$^{45}\text{Cl}$  beam  $\rightarrow {}^9\text{Be}(^{45}\text{Cl}, \text{xn}) {}^{54-\text{x}}\text{Sc}$

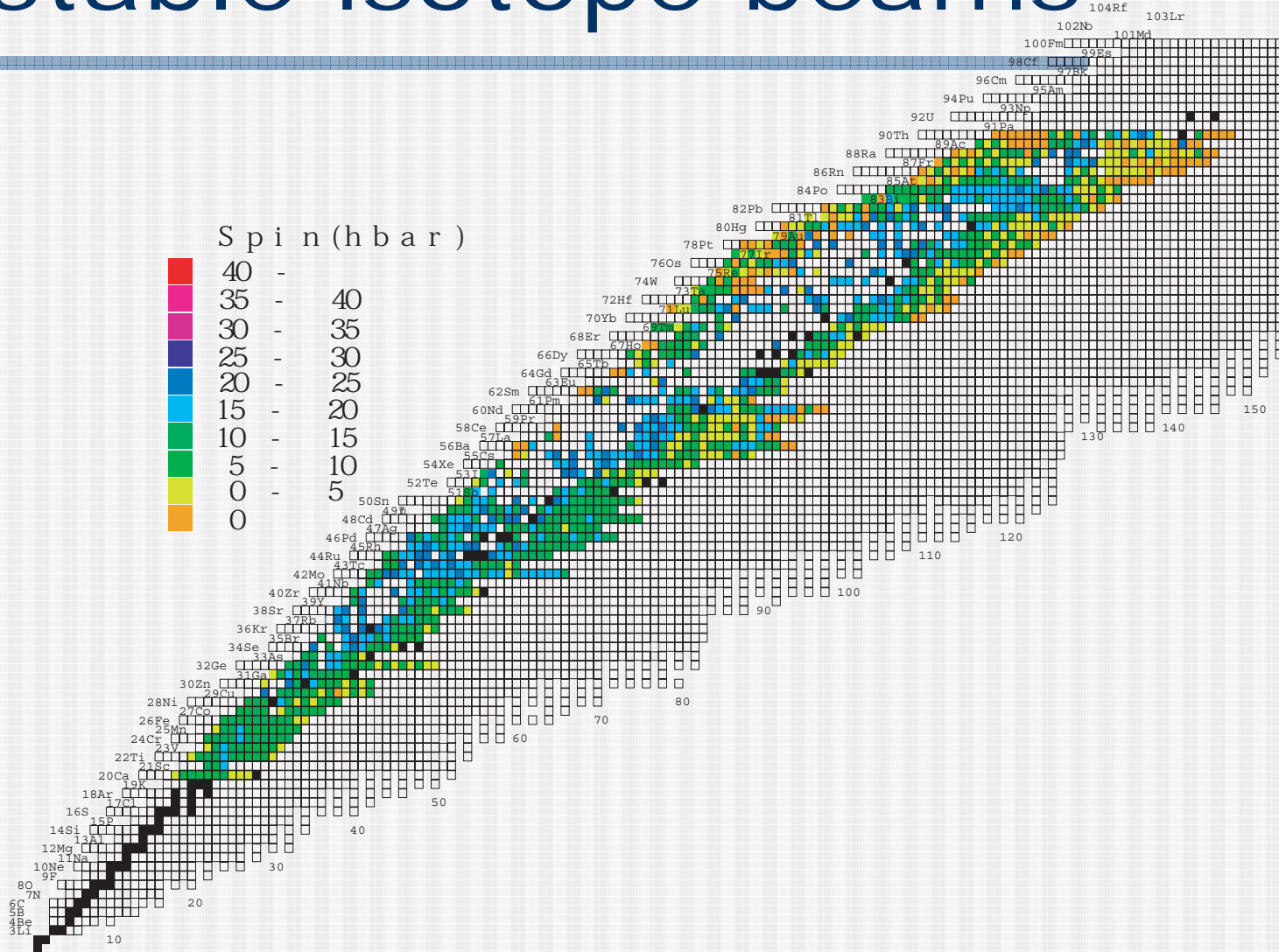
$^{67}\text{Co}$  beam  $\rightarrow {}^9\text{Be}(^{67}\text{Co}, \text{xn}) {}^{76-\text{x}}\text{Ga}$

- Multiple Coulomb excitation of low-energy RI beam

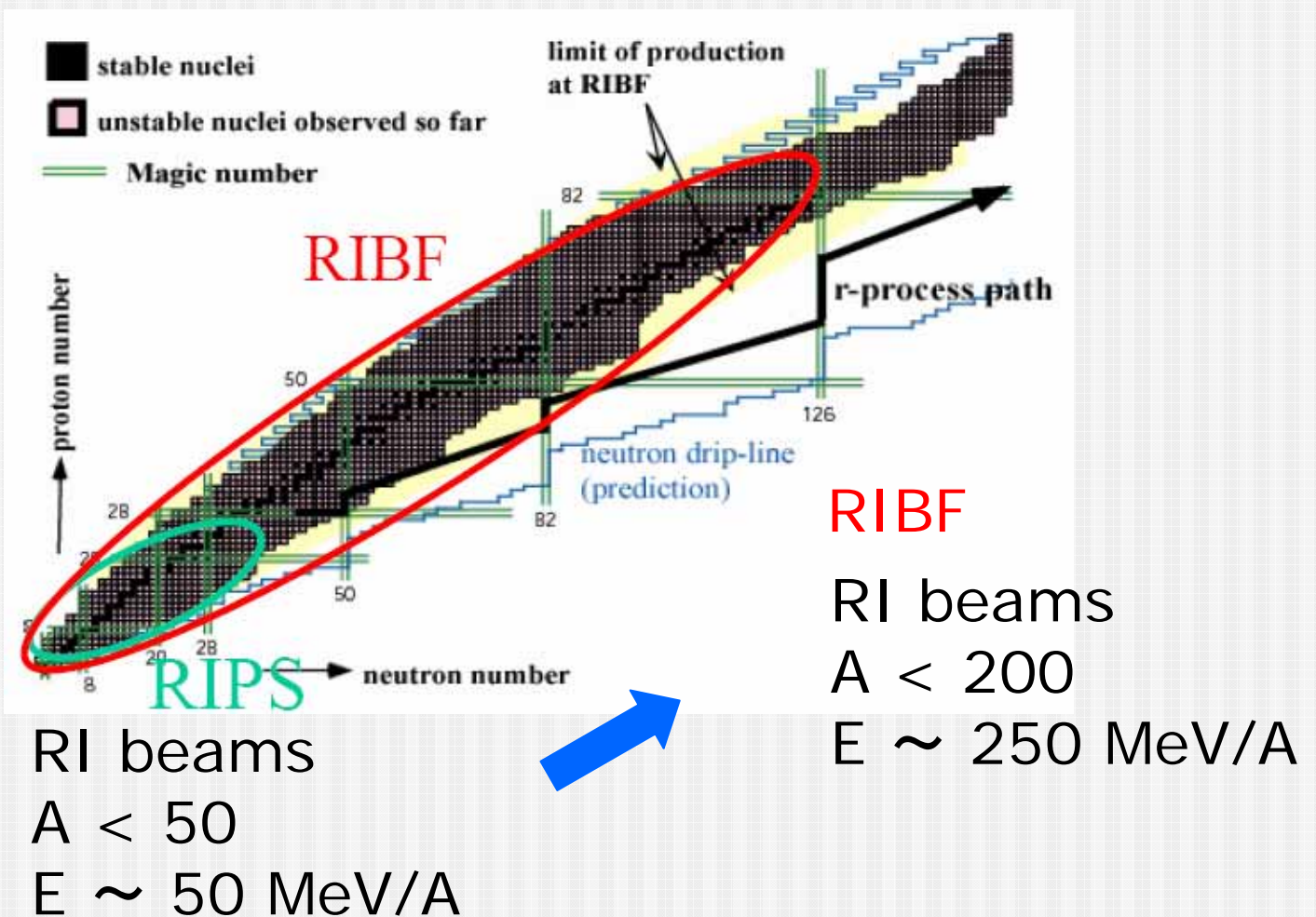
Neutron-rich deformed nuclei



# High-spin study using stable isotope beams



# RI Beam Factory



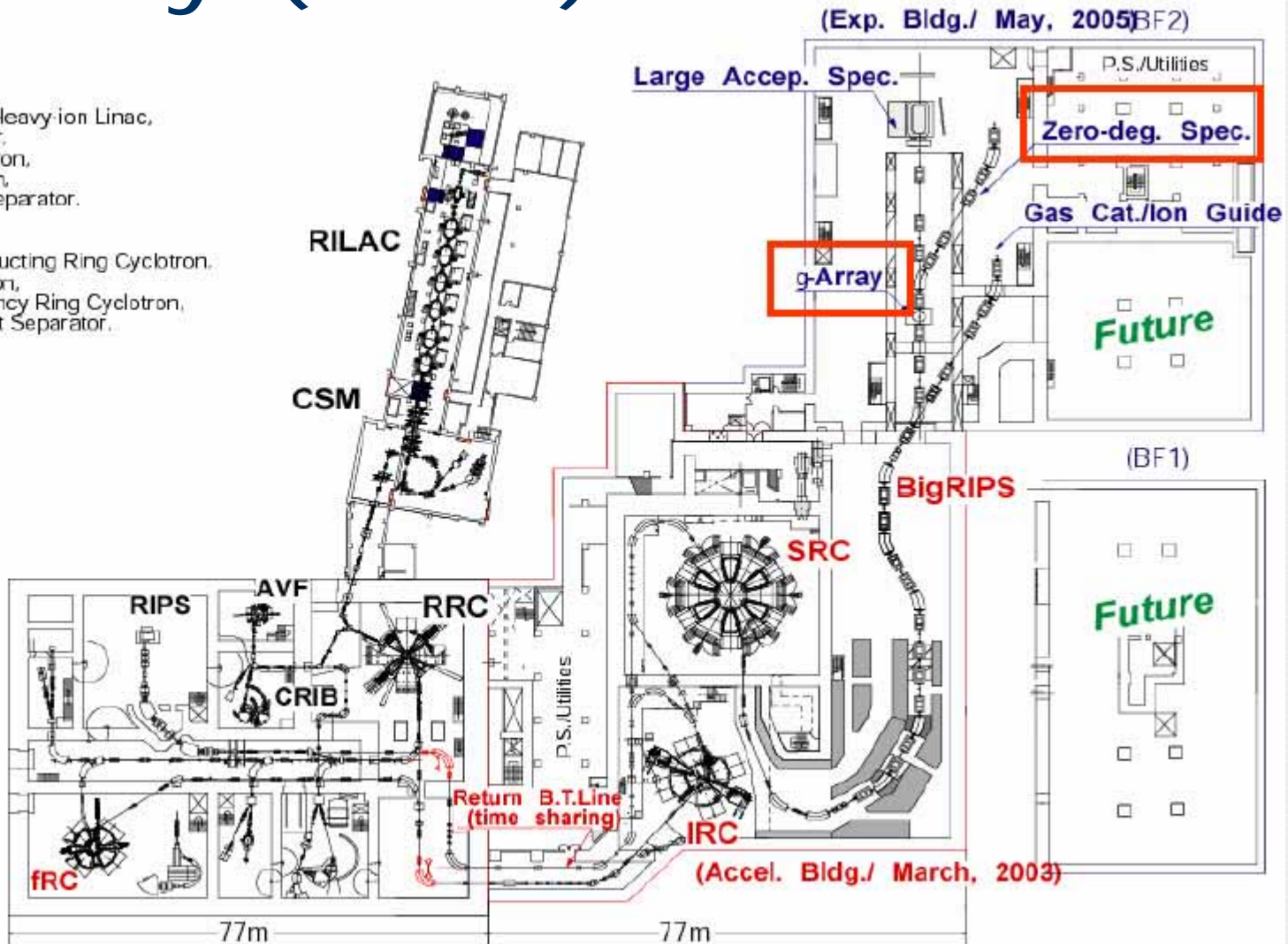
# Layout of the RI Beam Factory (RIBF)

## Existing Facility:

RILAC: Frequency-variable Heavy ion Linac,  
CSM: Charge State Multiplier,  
RRC: K540MeV Ring Cyclotron,  
AVF: K70MeV AVF Cyclotron,  
RIPS: Projectile Fragment Separator.

## RIBF Phase I:

SRC: K2500MeV Superconducting Ring Cyclotron,  
IRC: K980MeV Ring Cyclotron,  
fRC: K520MeV Fixed frequency Ring Cyclotron,  
BigRIPS: Projectile Fragment Separator.



# Reactions for in-beam $\gamma$ -ray spectroscopy at RIBF

---

- Intermediate energy RI-beams ( $\sim 250 \text{ MeV/A}$ )
  - Coulomb excitation,
  - Proton inelastic scattering,
  - Fragmentation
  - Knock-out reaction
  
- Deceleration with materials ( $5 \sim 30 \text{ MeV/A}$ )
  - Transfer reactions
  - Deep inelastic reactions
  - Multiple Coulomb excitation
  - Fusion reaction

---

End